Cross-Scale Air-Sea Interaction in the Tropics

Chidong Zhang
RSMAS, University of Miami

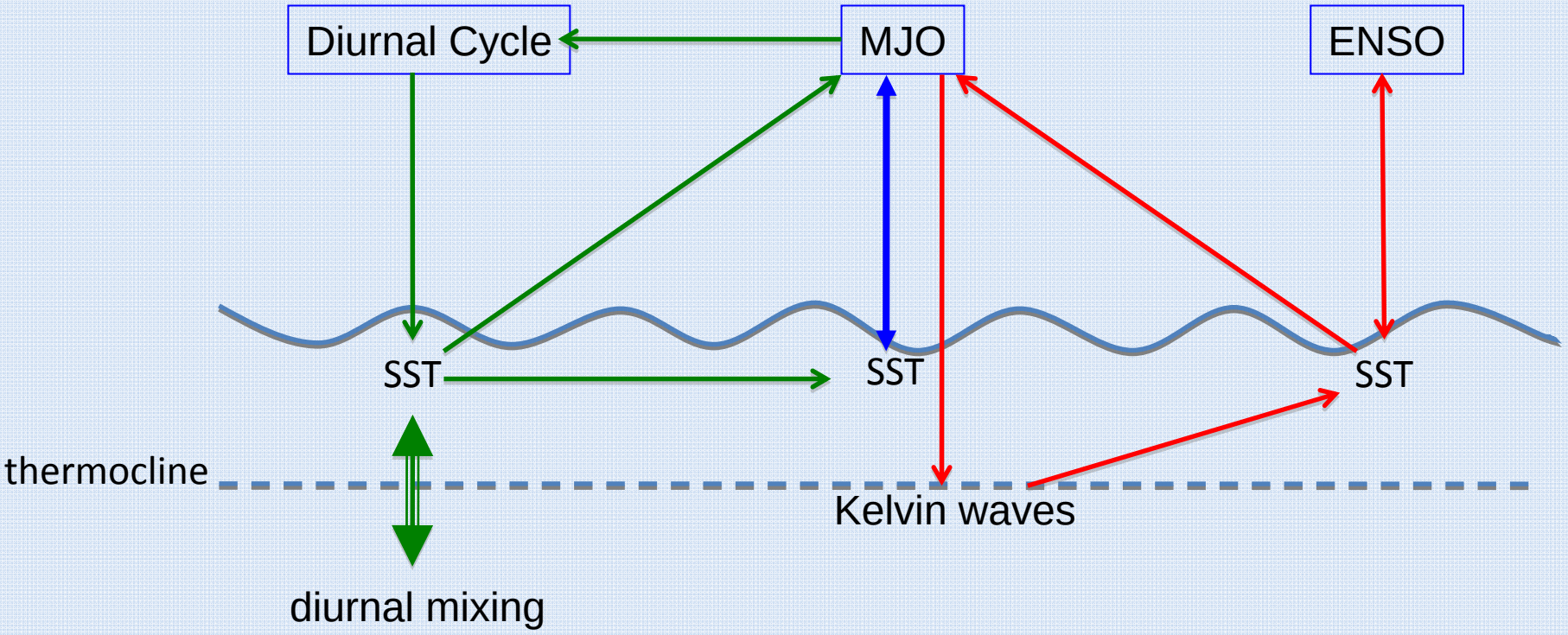

Air-Sea Interaction Connecting the MJO and Diurnal Cycle

Issues:

- **Importance of the MJO structure (phase relationships among its surface forcing)**
- **Importance of buoyancy flux (sensitivity of SST to precipitation)**

Structural Models of the MJO

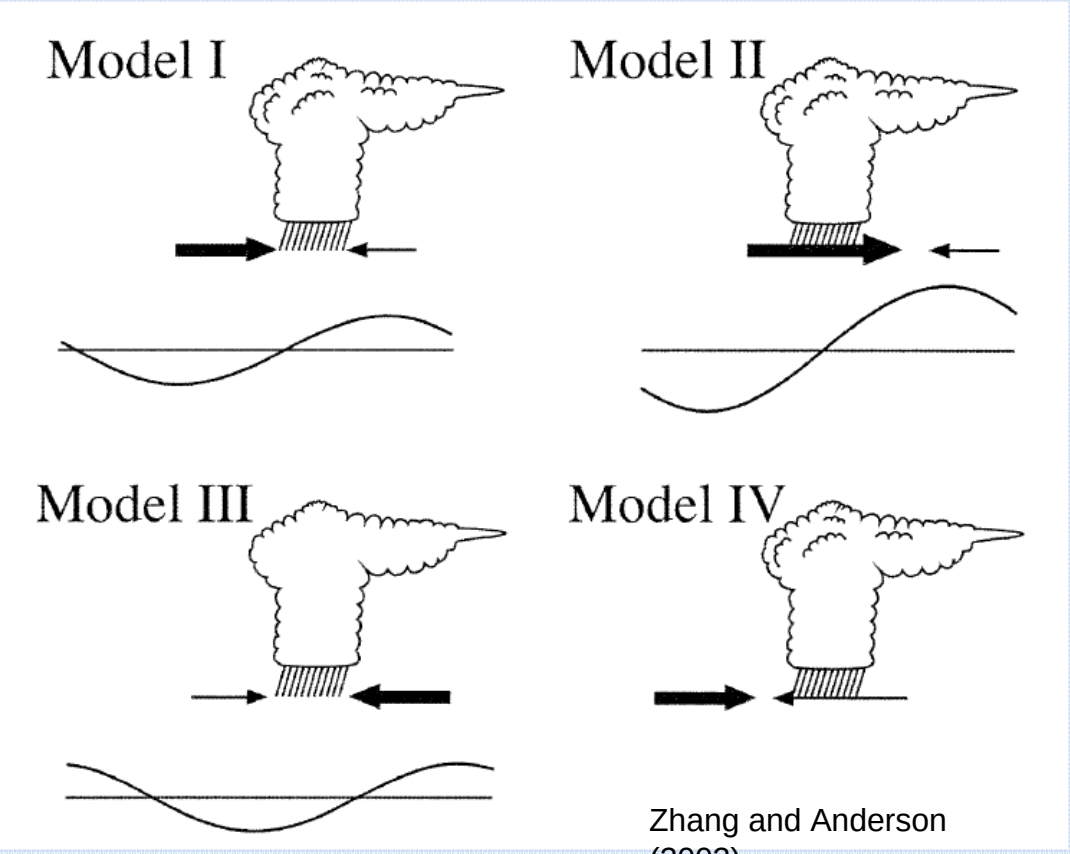

Zhang and Anderson (2003)

Observations (W. Pacific)
- strongest net surface heat flux
- large cancelation among buoyancy flux components
- weak SST sensitivity to precip

Numerical/Theoretical Models
- weakest net surface heat flux
- small cancelation among buoyancy flux components
- strongest SST sensitivity to precip

Sensitivity of Intraseasonal SST Perturbations to the MJO Structure

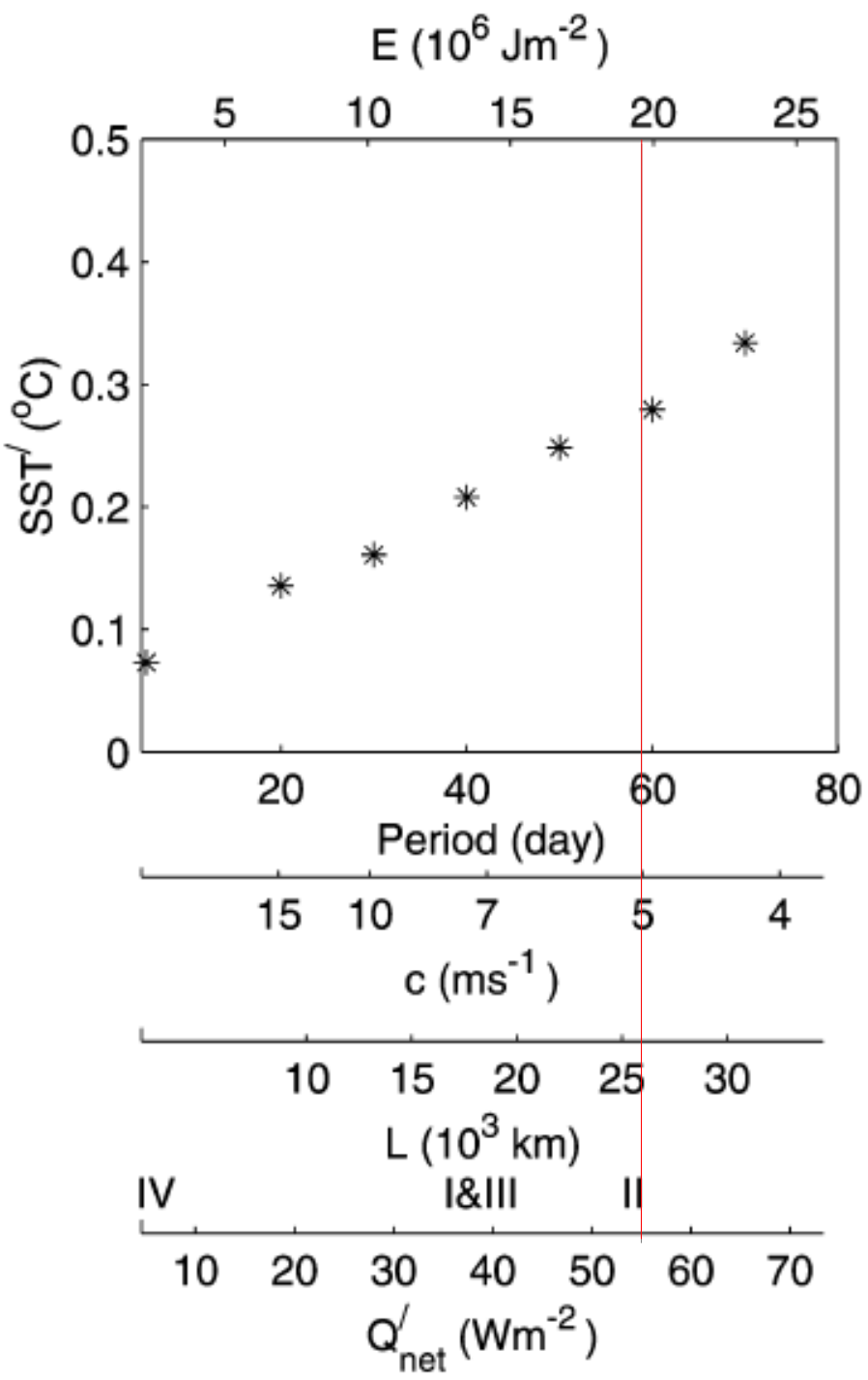

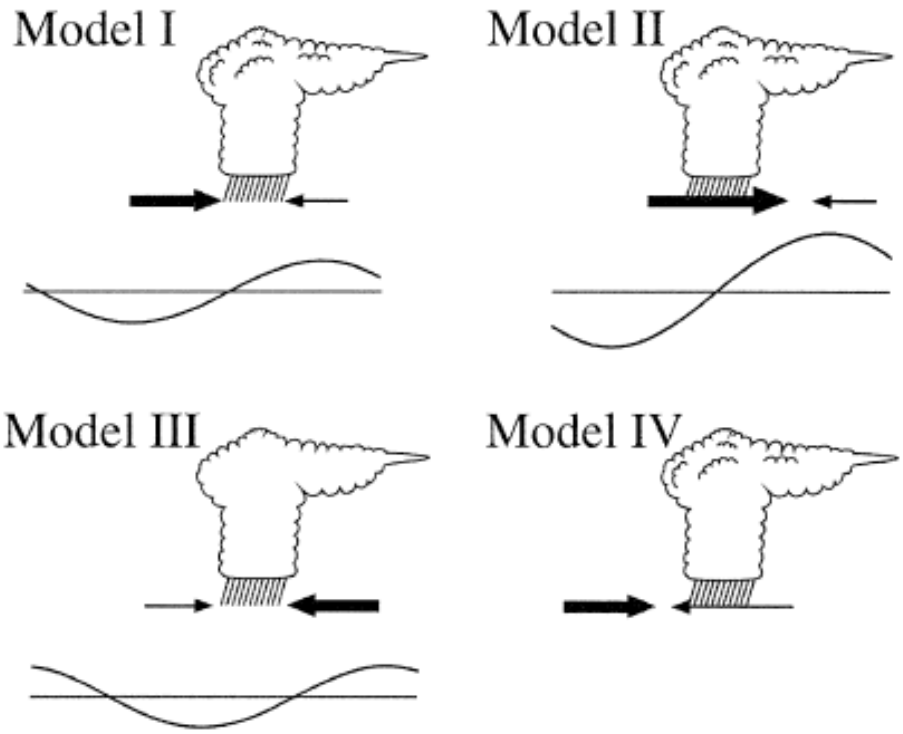

$$B_{net} = B_{heat} + B_{precip} - B_{evap} = \alpha(C_p\rho)^{-1}Q_{net} + \beta S_0(P\text{-}E)$$

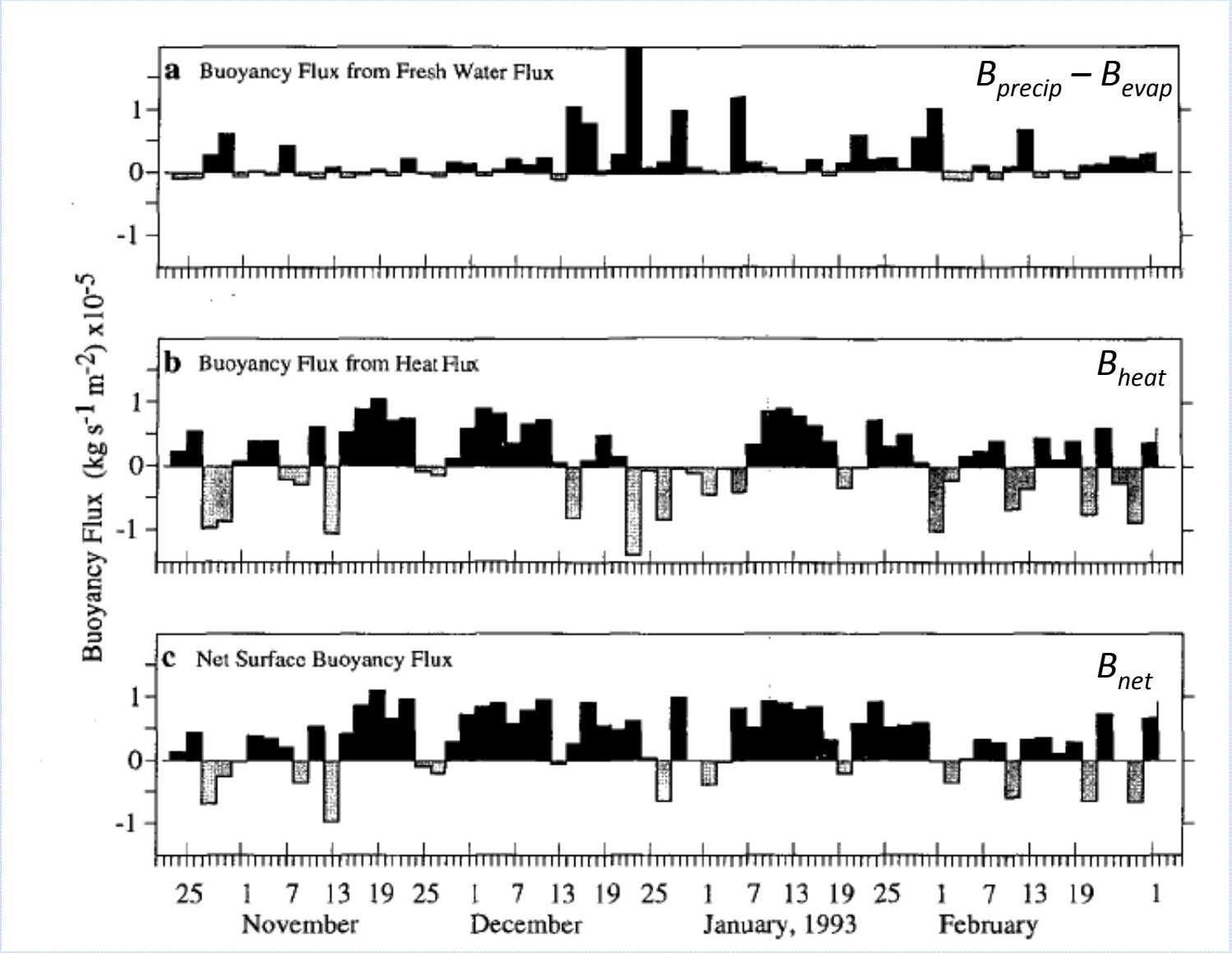

Anderson et al (1996)

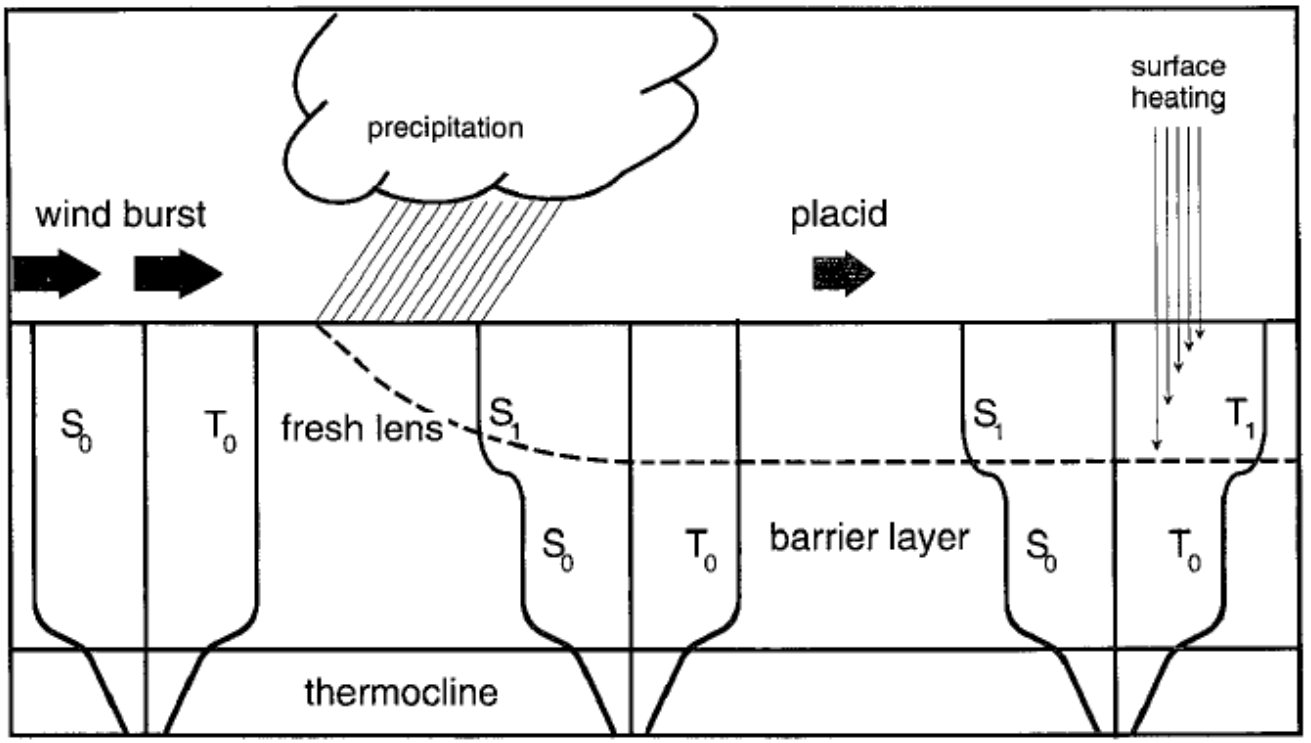

FIG. 2. Schematic diagram showing the Lukas–Lindstrom ''barrier layer'' theory. During a strong wind burst, the surface mixed layer extends down to the top of the thermocline. Following the wind burst, the additional buoyancy from precipitation and strong surface heating acts to form a relatively warm and fresh thin surface mixed layer. Below this thin layer is a strong halocline, which effectively decouples the surface forcing from the deeper waters. Further heating is trapped to vertical mixing above the barrier formed by the halocline.

Anderson et al (1996)

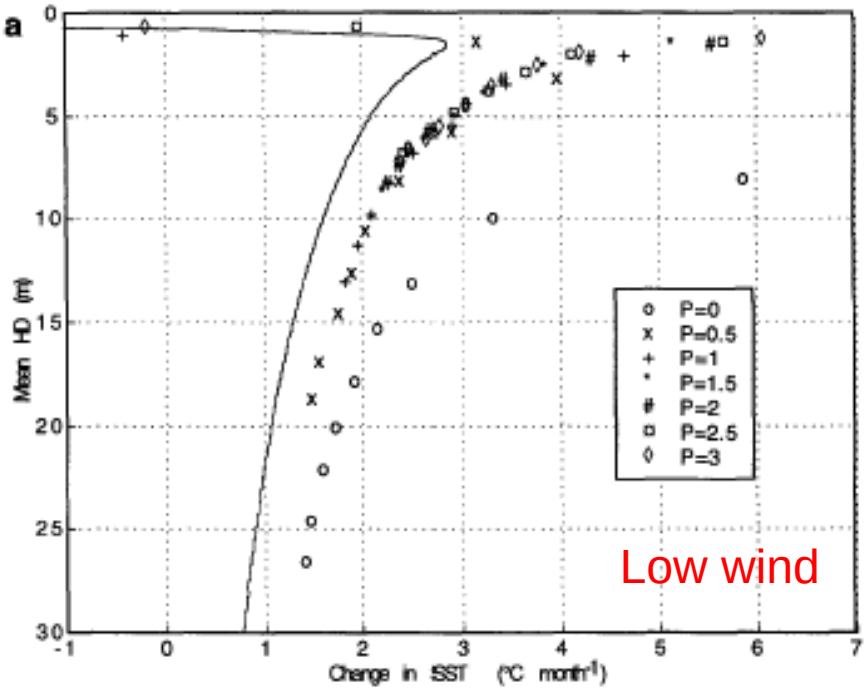

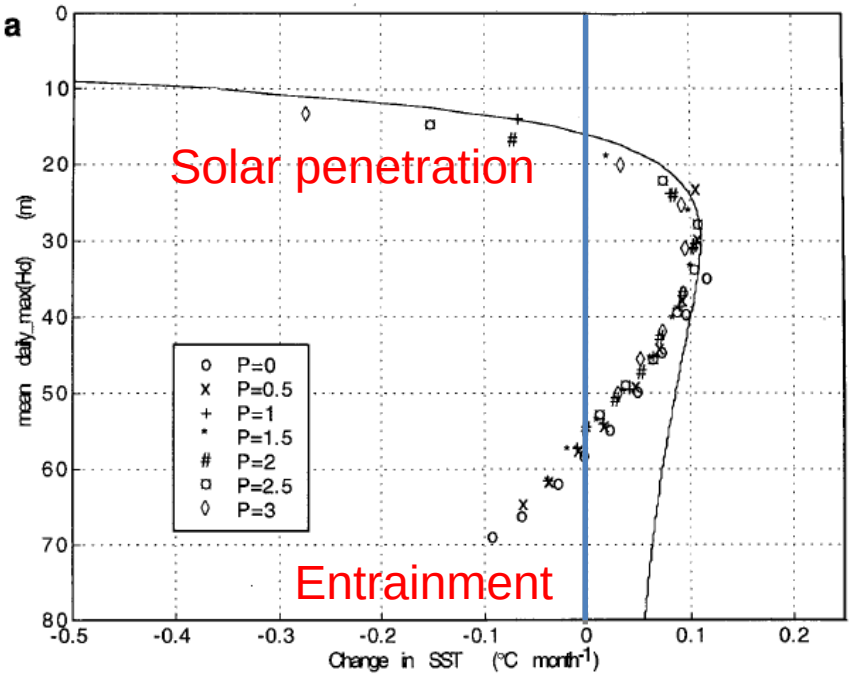

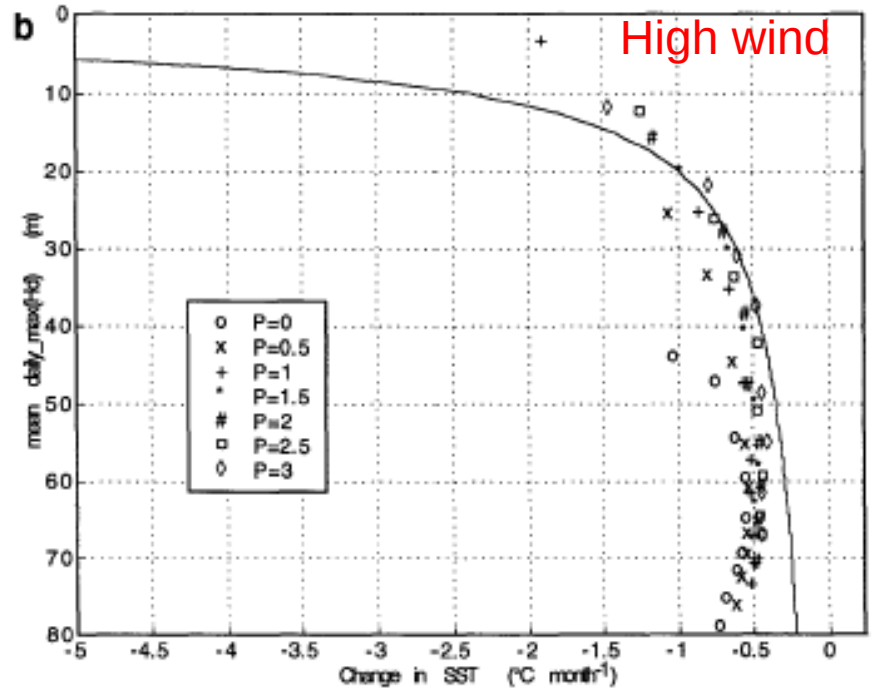

Anderson et al (1996)

Sensitivity of Intraseasonal SST Perturbations to Precipitation

x: strong wind stress
+: weak wind stress
o: weak wind stress + enhanced mean precipitation
∆SST': MJO SST sensitivity to MJO precipitation

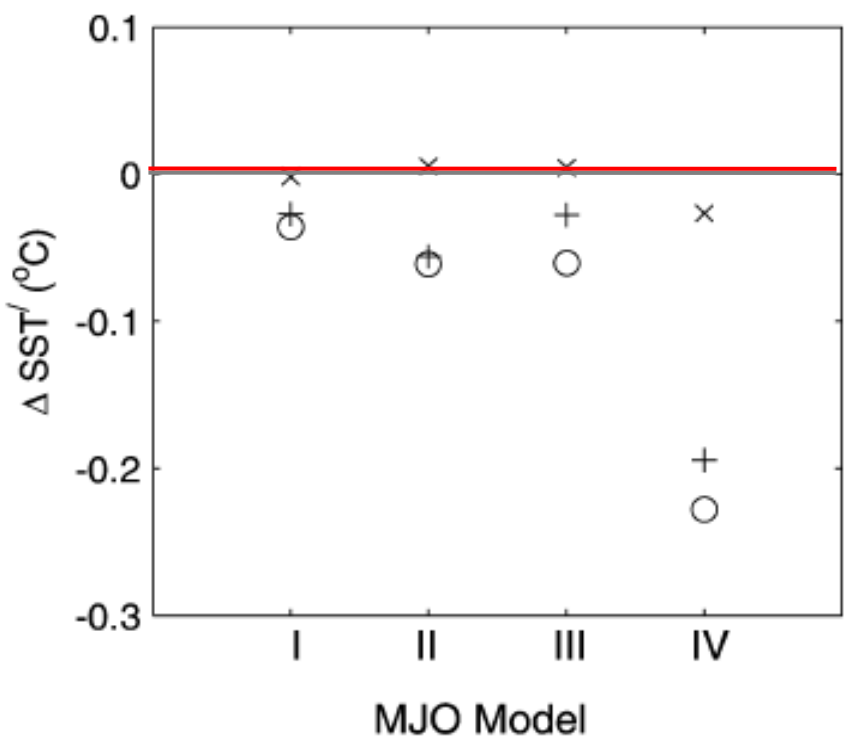

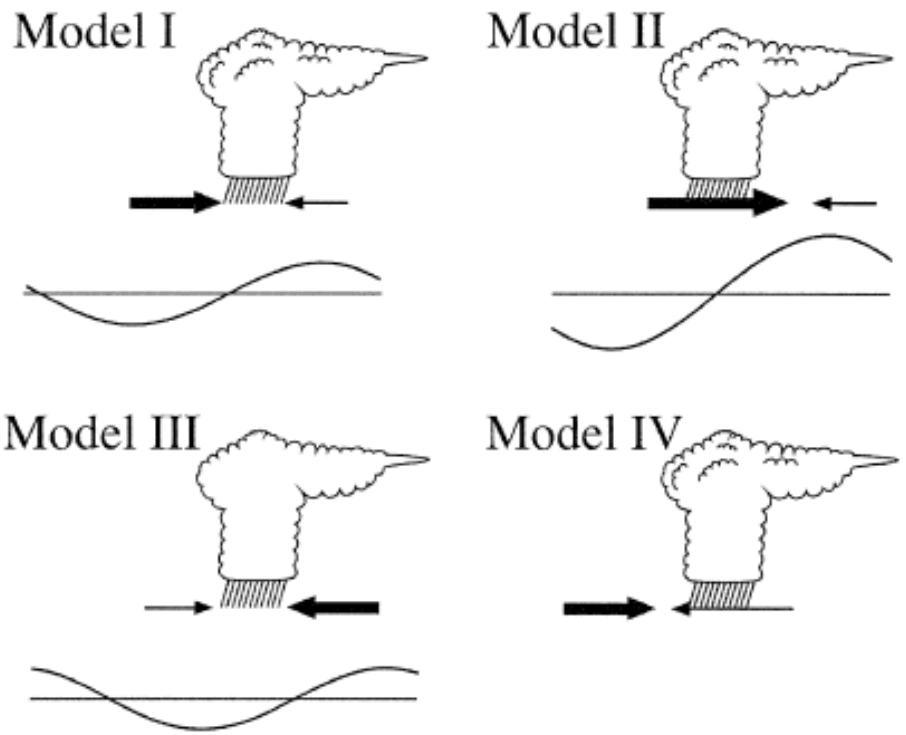

Zhang and Anderson (2003

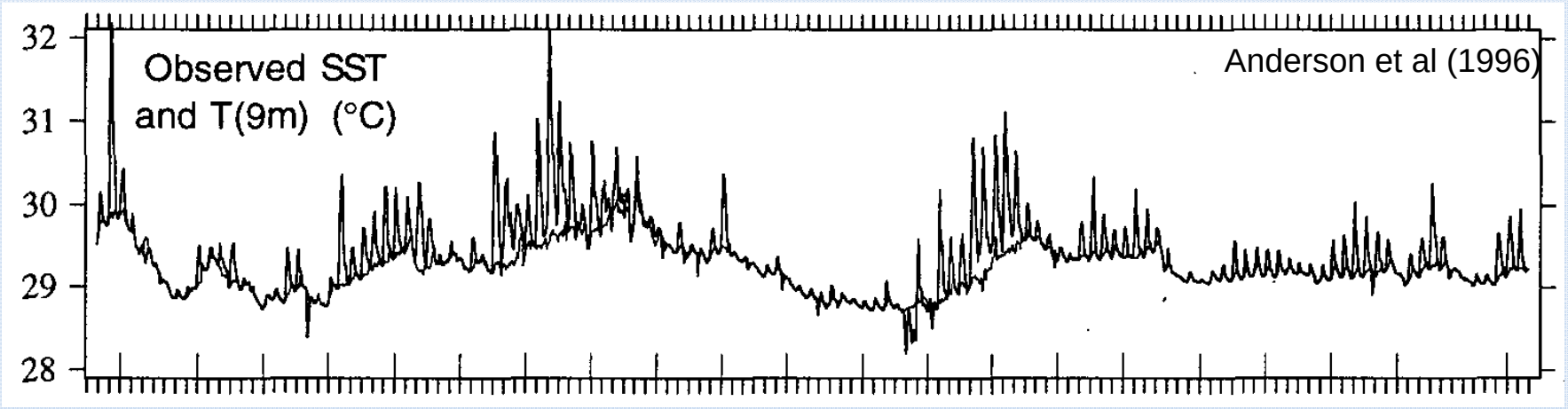

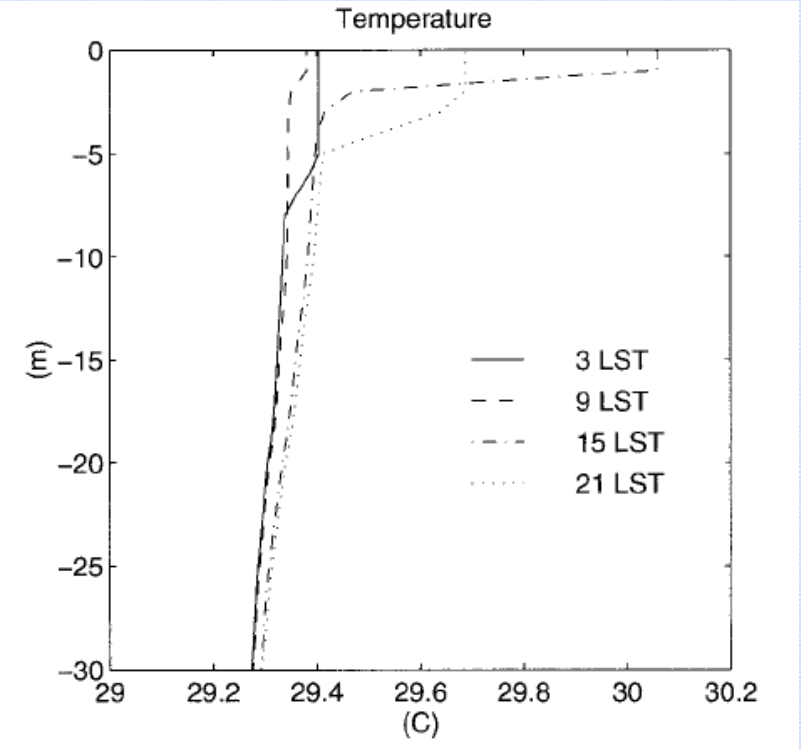

Shinoda and Hendon (1998)

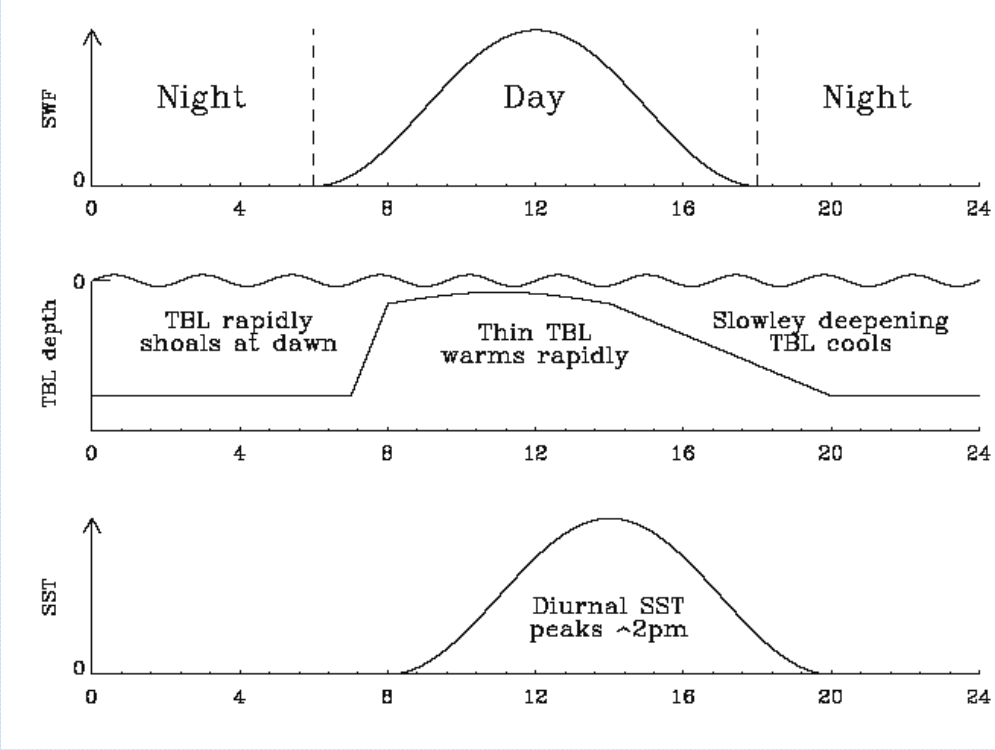

Bernie et al. (2005)

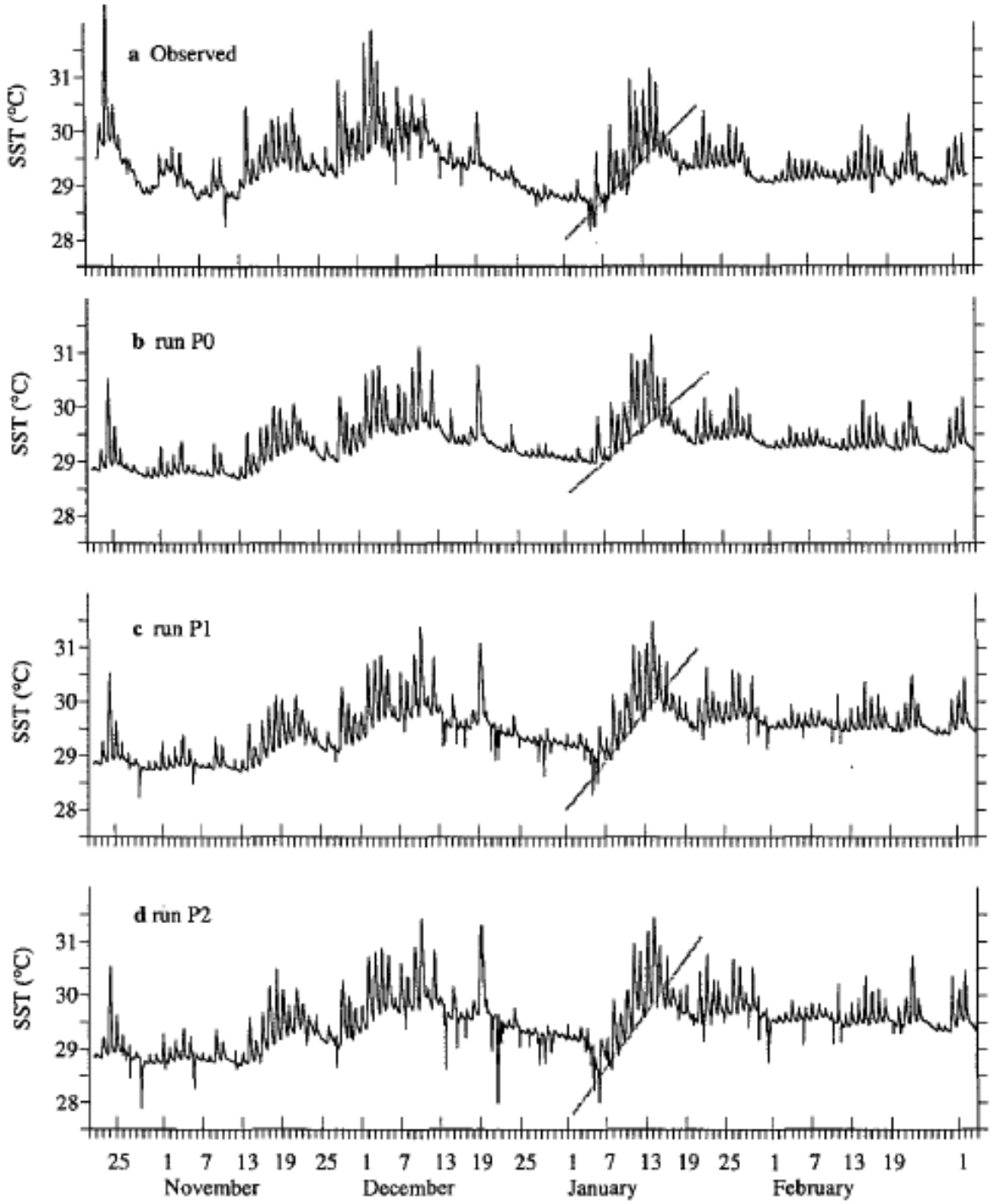

Anderson et al (1996)

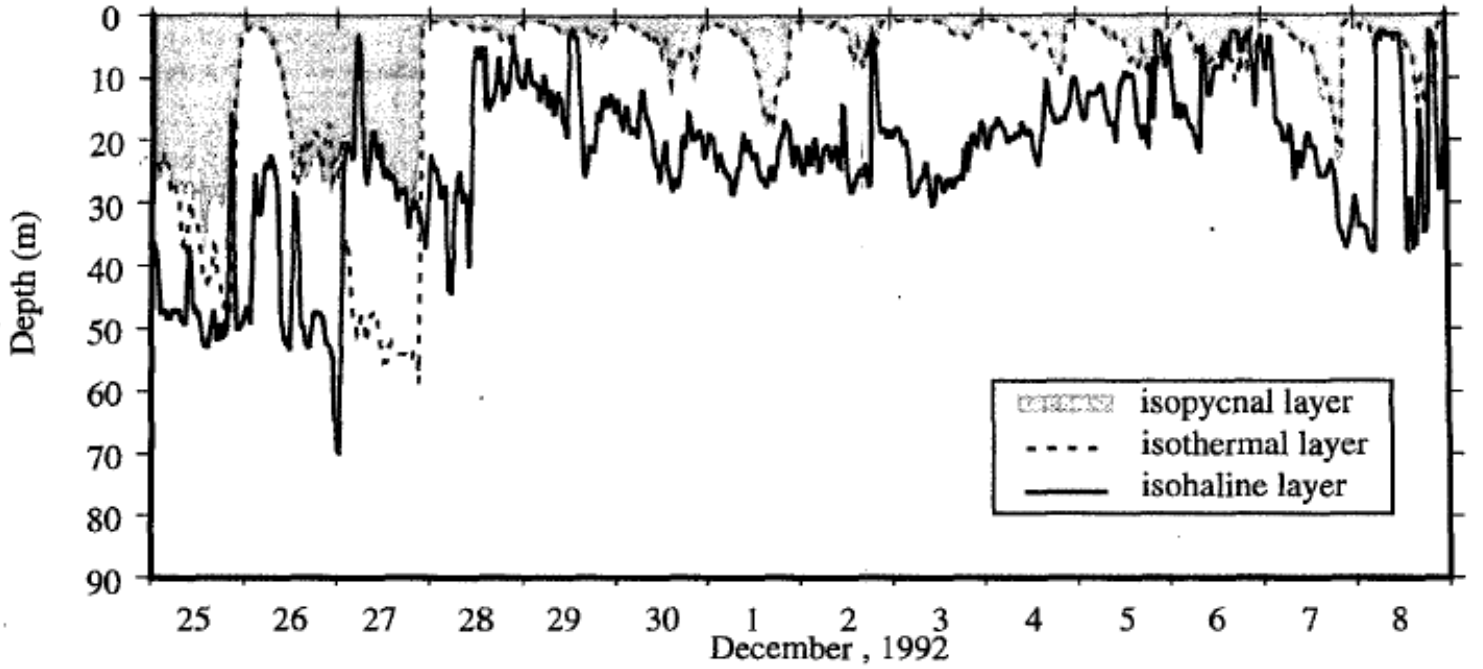

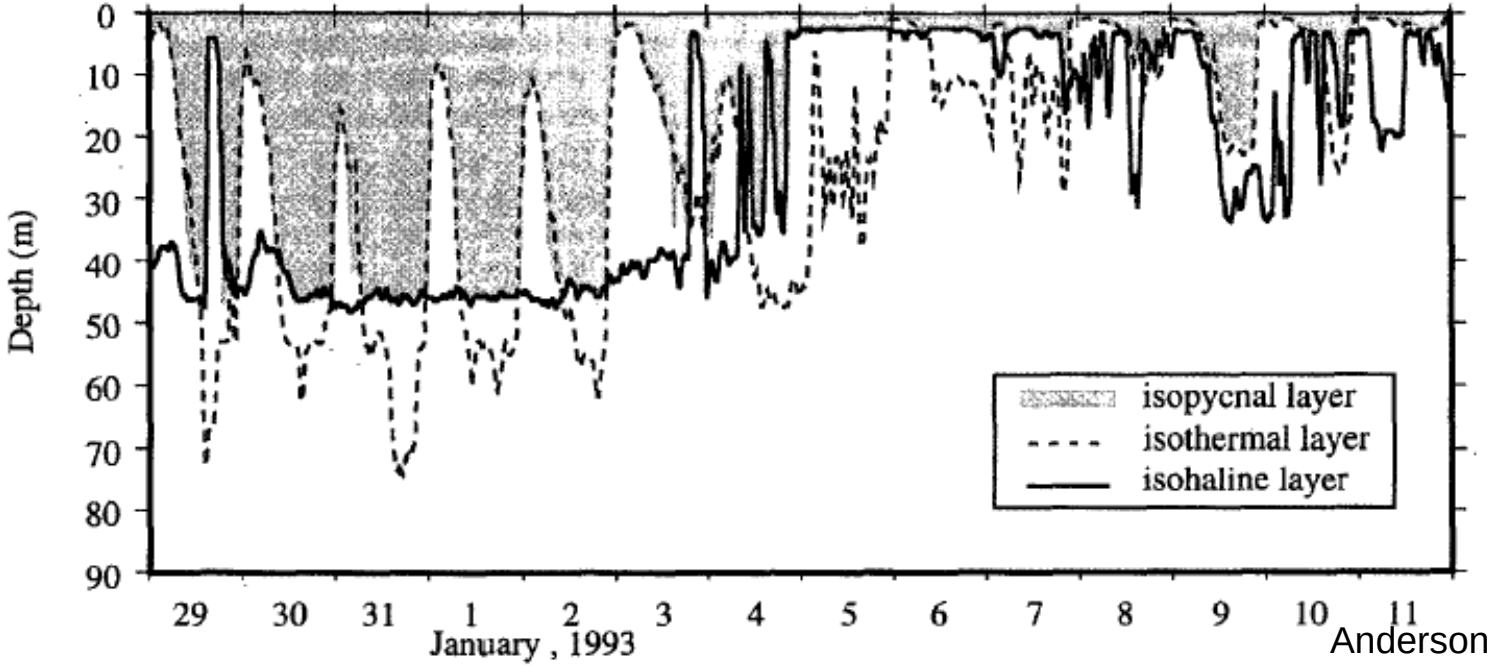

Anderson et al (1996)

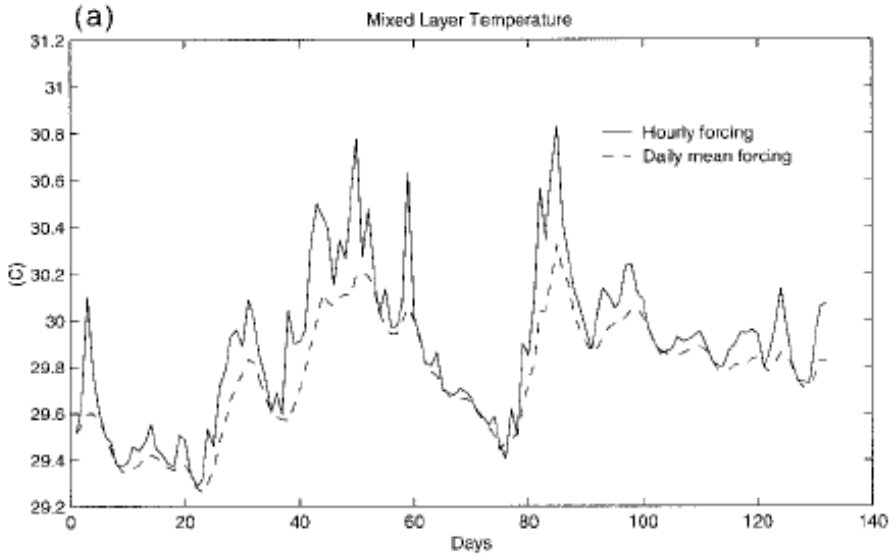

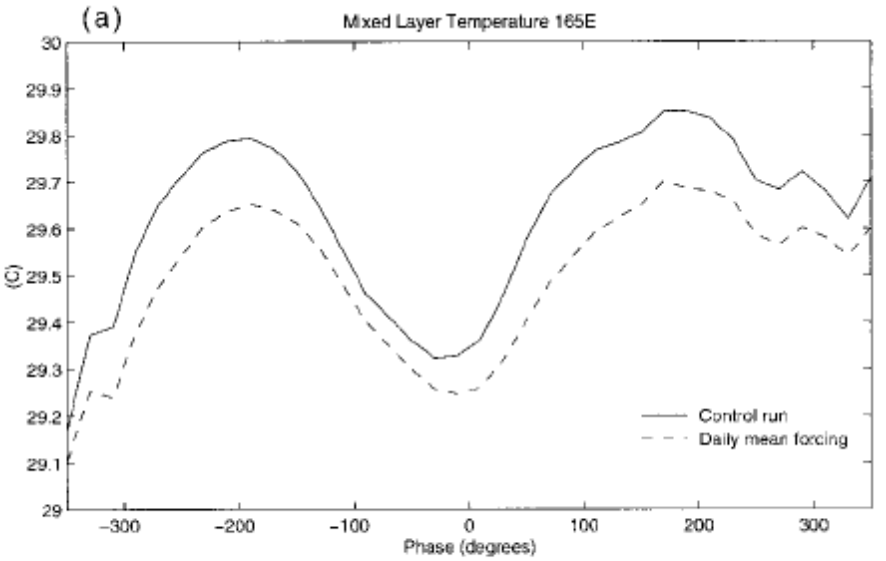

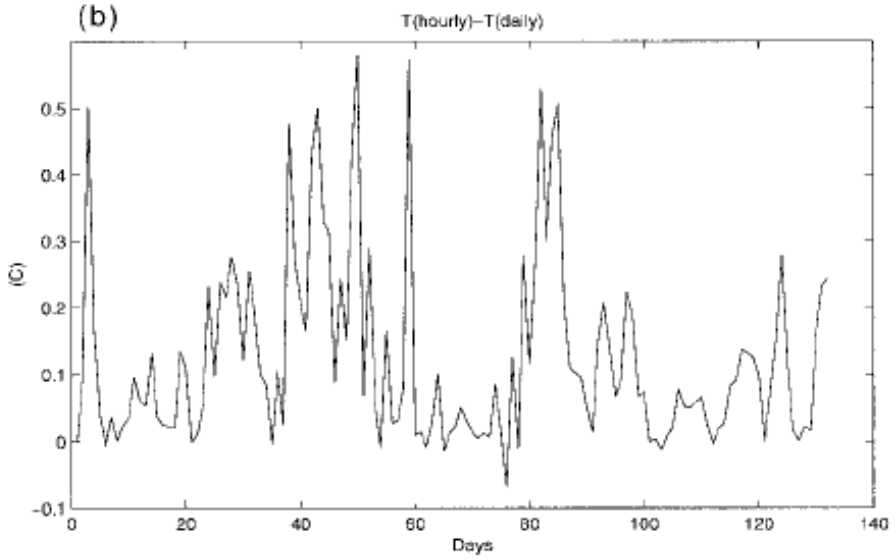

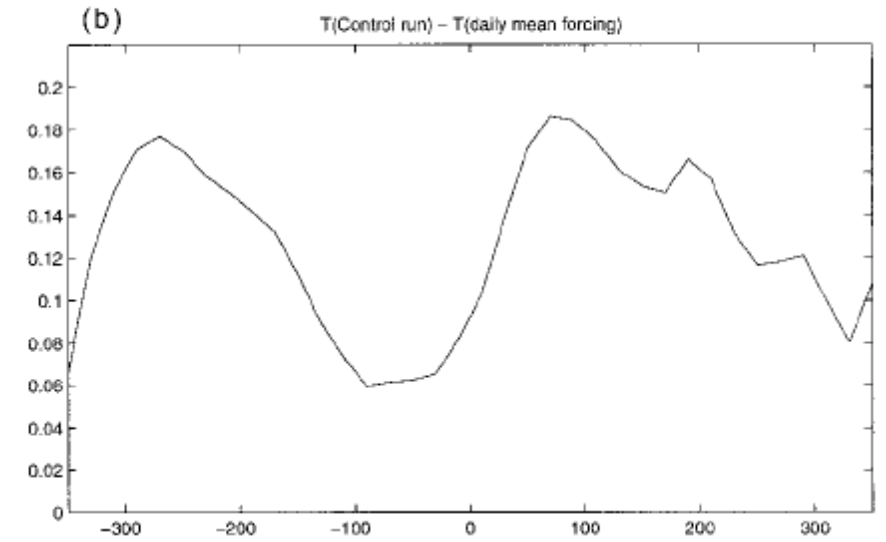

Shinoda and Hendon (1998)

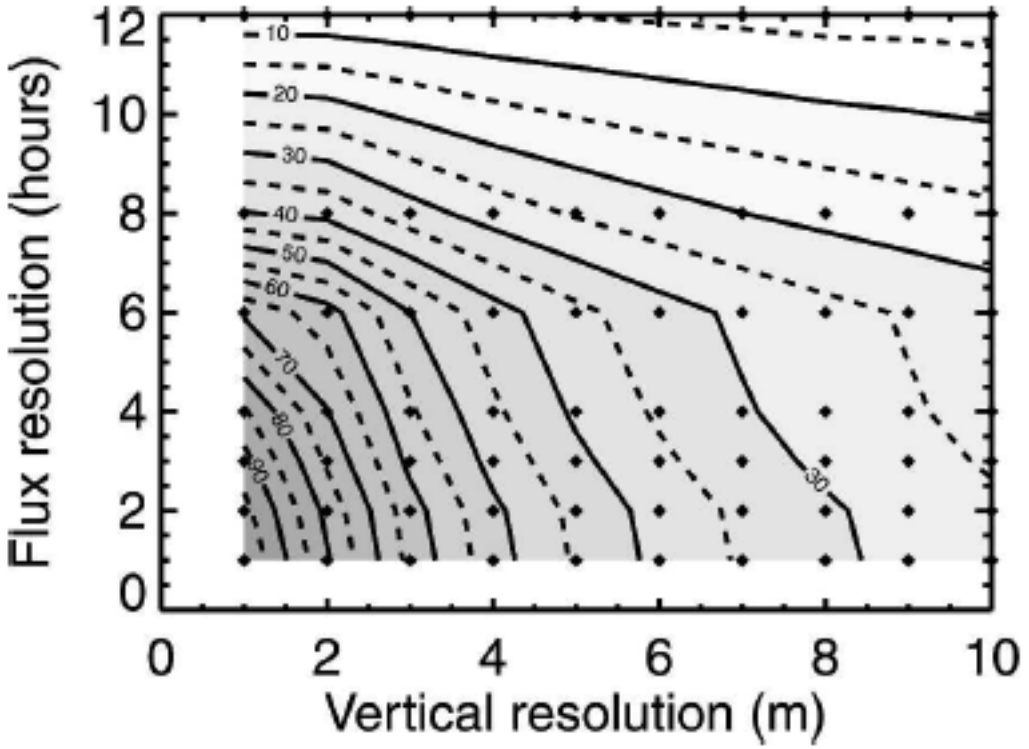

FIG. 14. Phase diagram showing the diurnal SST variability as a function of flux resolution and vertical resolution of the uppermost model level. Contours show the percentage of the magnitude of the diurnal variability in the control integration CTL. For the flux resolution, the results from the least optimal averaging period are used, that is, the lower limits of the bars shown in Fig. 7.

Bernie et al. (2005)

Interaction between the MJO and ENSO

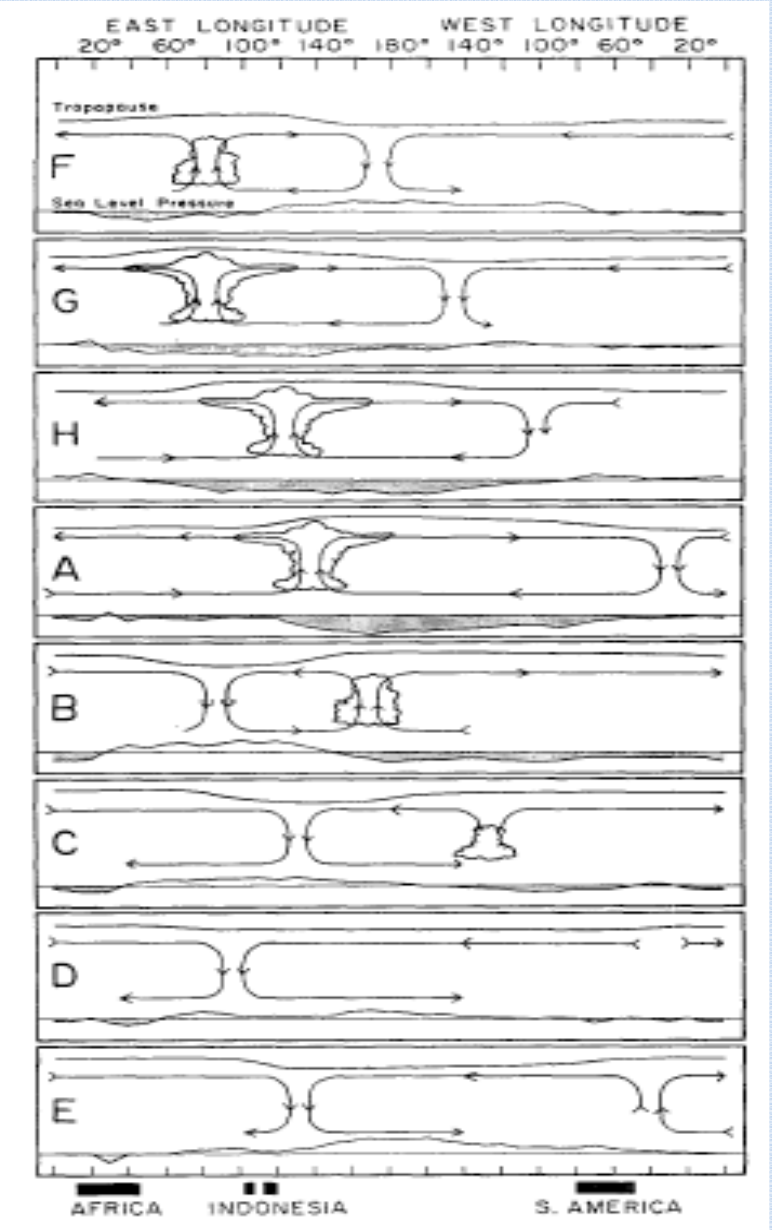

?

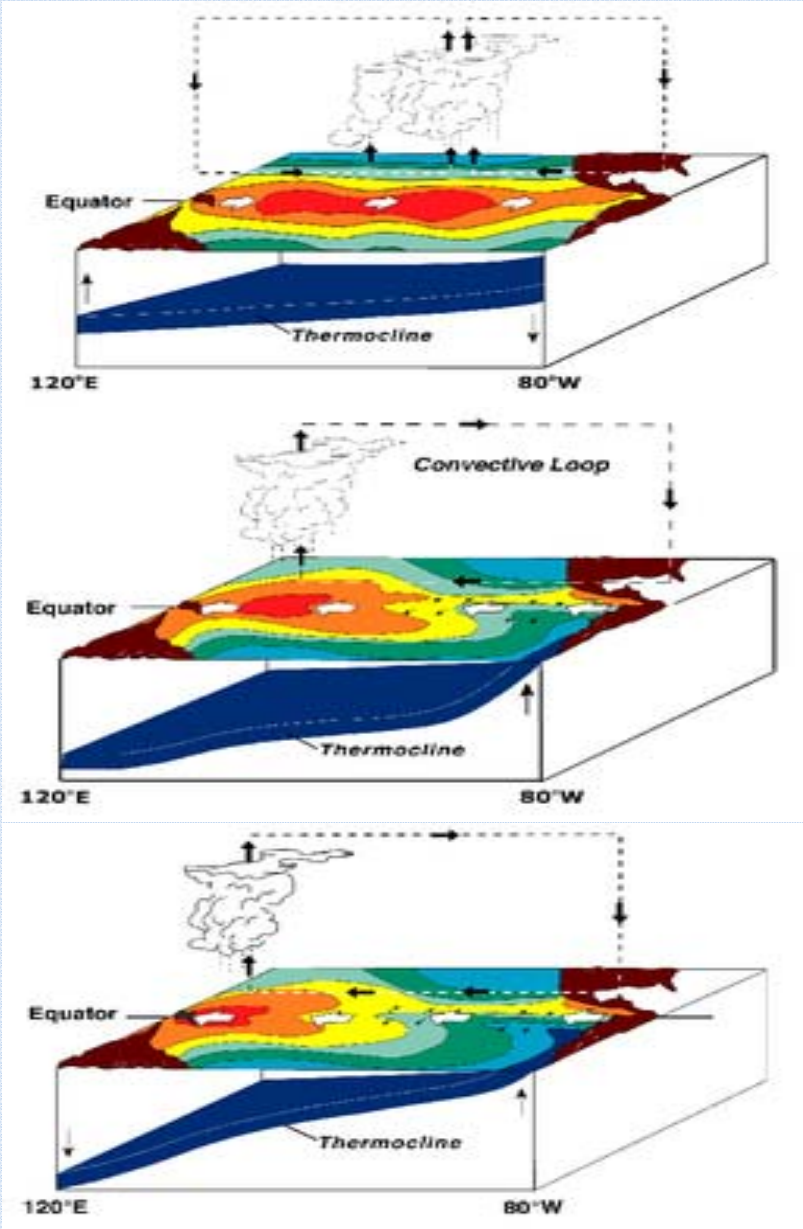

Stochastic forcing of climate variability (Hasselmann 1976):

$$z = s + f$$

$$df/dt = P(f, s_0)$$

$$ds/dt = W(s) + G(f)$$

P: high-frequency dynamics

Ω: low-frequency dynamics

G: stochastic forcing dynamics

For ENSO:

s = SST

$f = \tau_x$

W*: delayed oscillator; energy discharge-recharge; ….*

P*: MJO dynamics (?)*

G(f) *= [M(SST)+A]f*

M=0: additive stochastic forcing

M≠0: mulpiplicative stochastic forcing

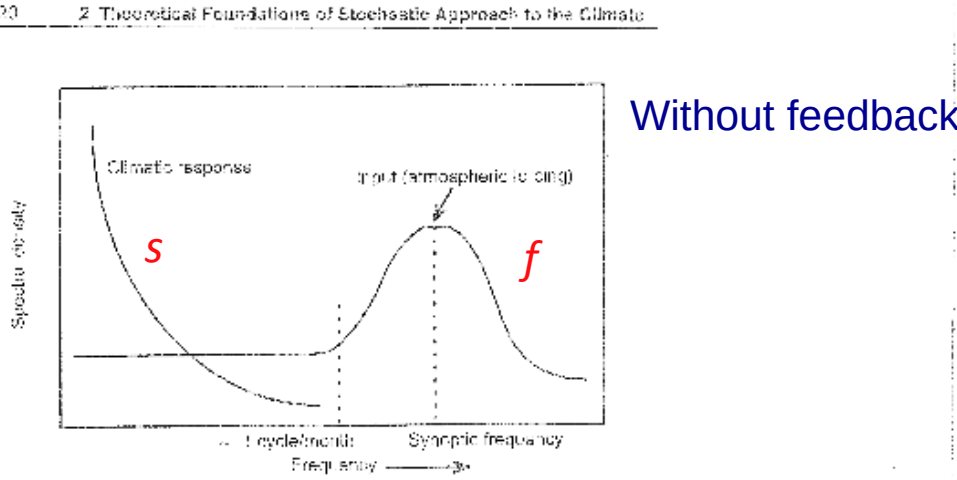

Without feedback

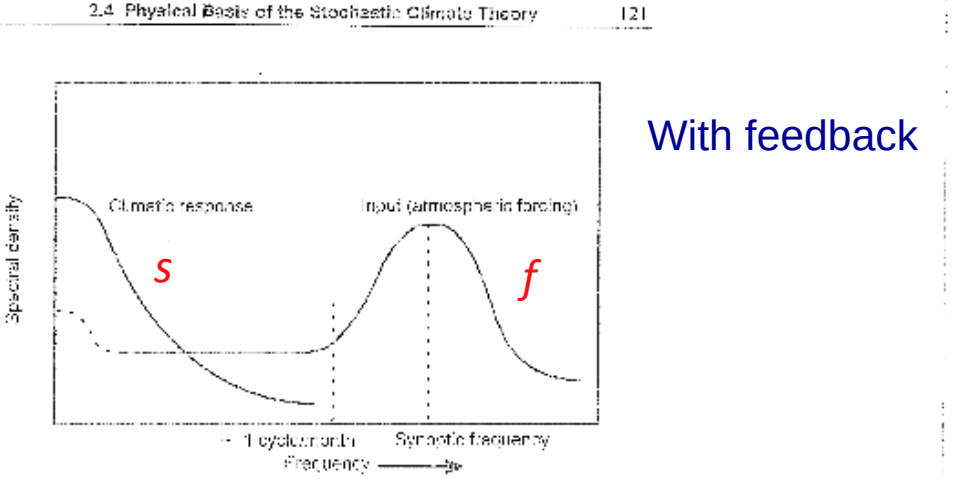

With feedback

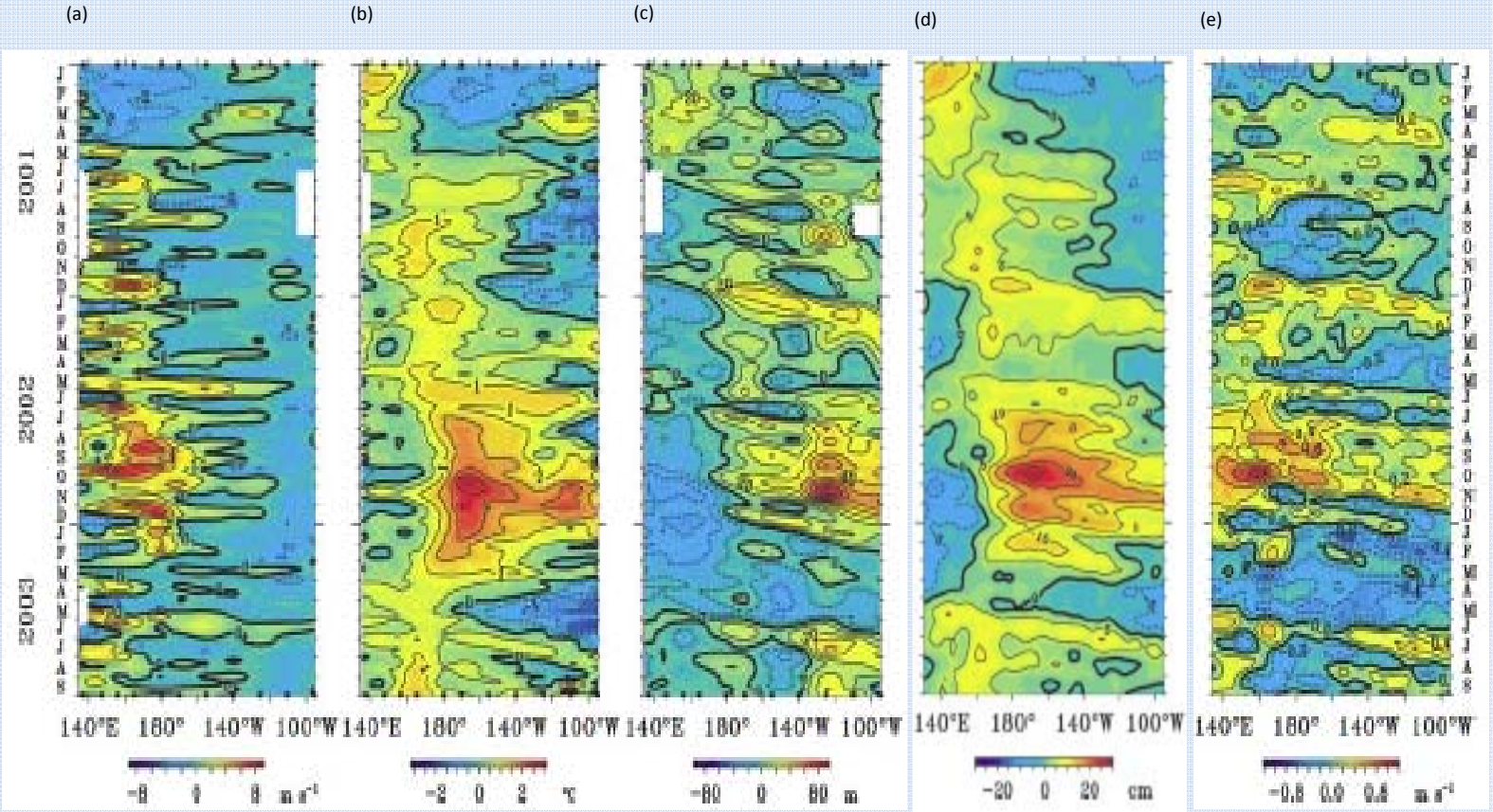

Anomalies of (a) zonal wind, (b) SST, and (c) 20°C depth (an index for the depth of the thermocline), (d) sea surface height, and (e) zonal current velocity averaged between 2°N–2°S relative to the mean seasonal cycle for January 2001 - September 2003. (From McPhaden 2004)

$$\tau_n = \tau_{MJO} + \tau_{NMJO}$$

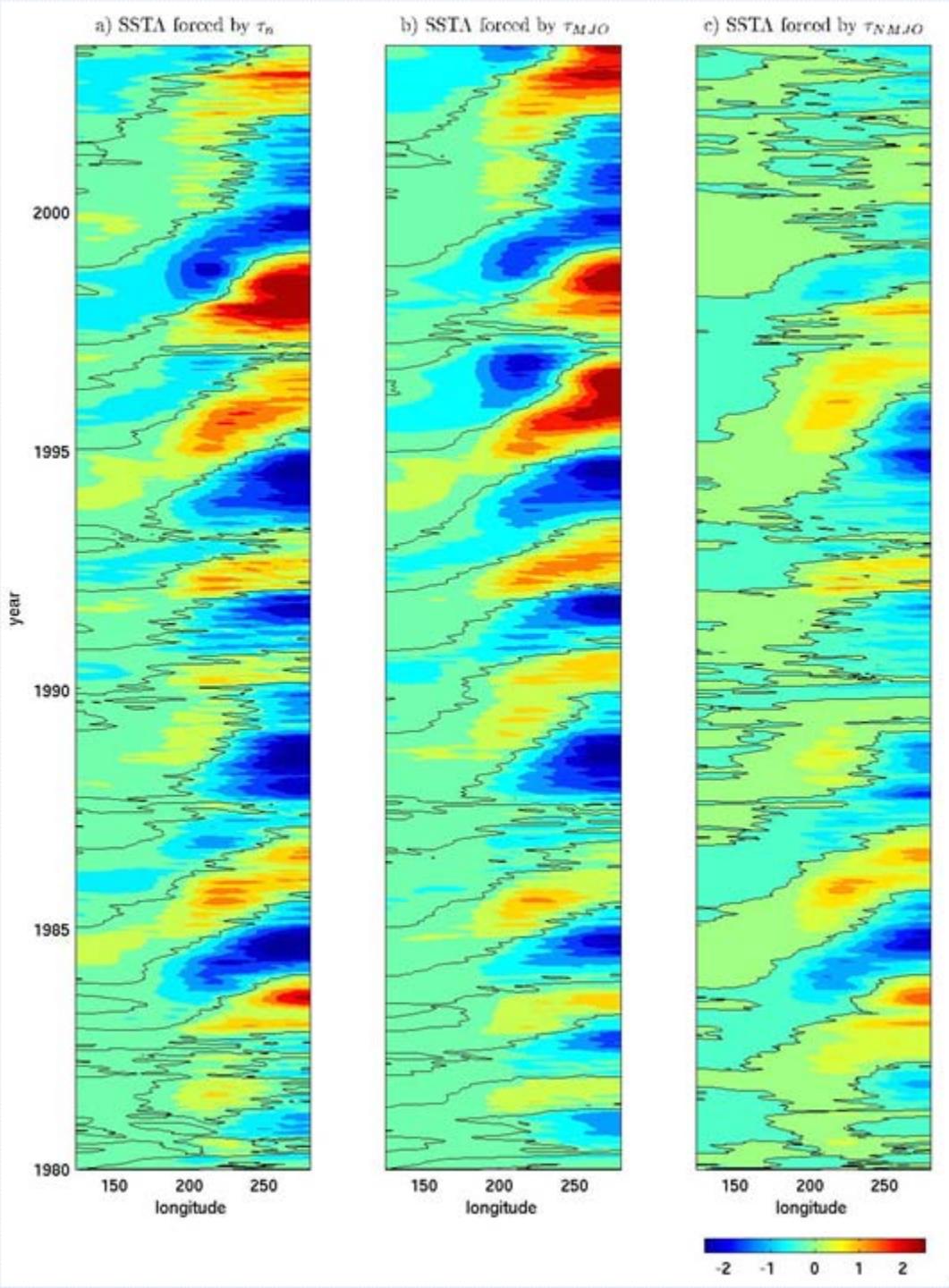

Zavala-Garay et al 2005

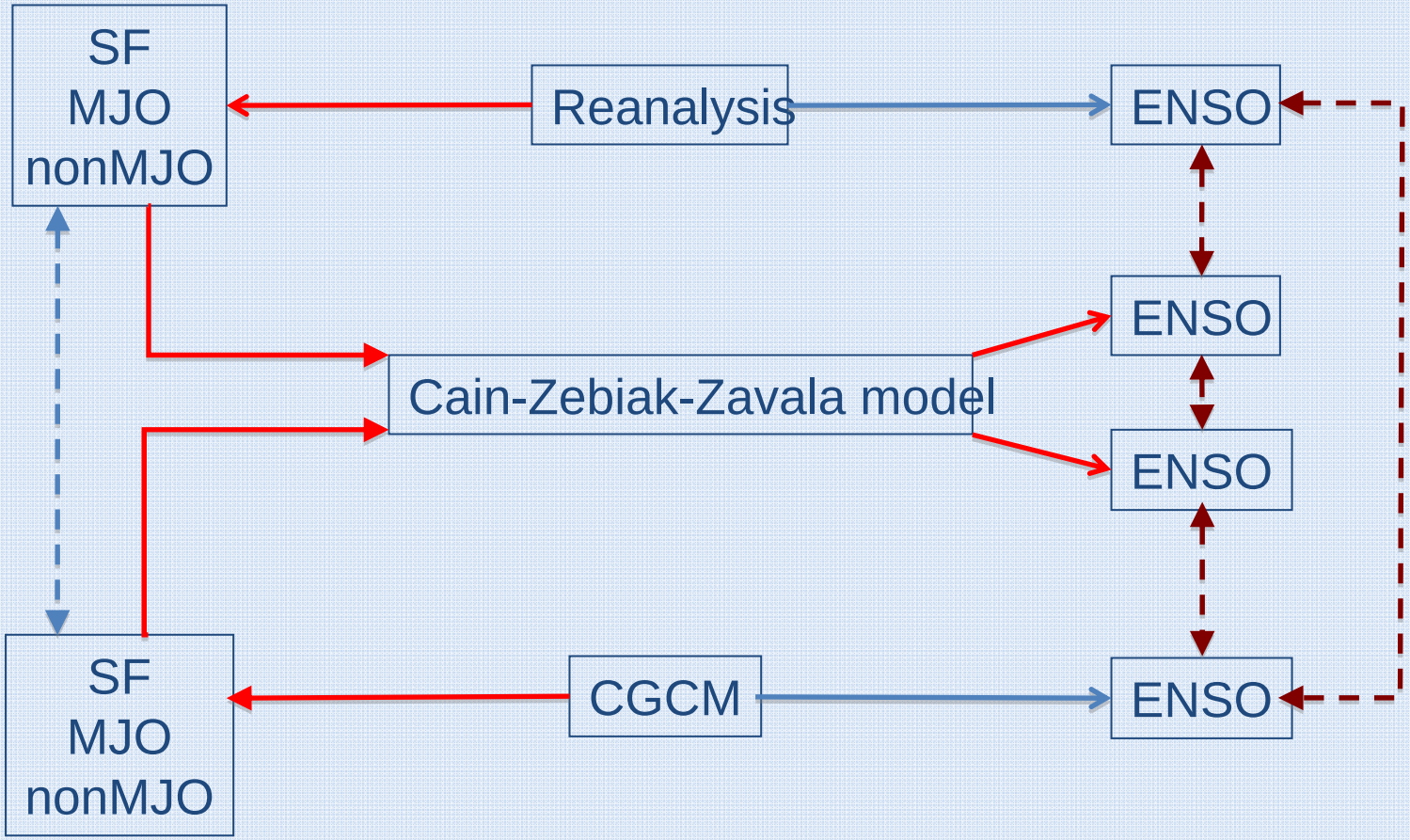
SF
MJO
nonMJO
Reanalysis
ENSO
ENSO
Cain-Zebiak-Zavala model
ENSO
SF
MJO
nonMJO
CGCM
ENSO

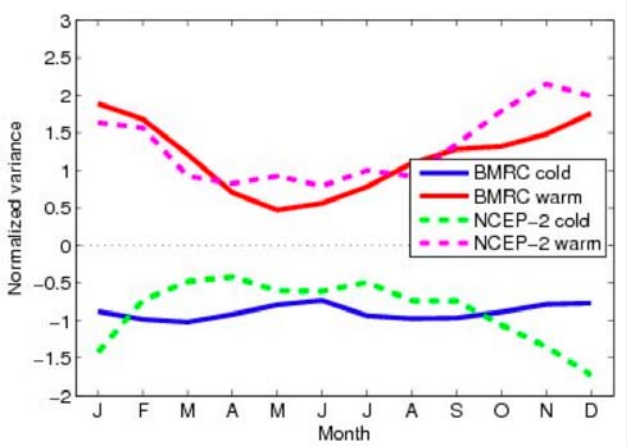

CZZ + NCEP SF

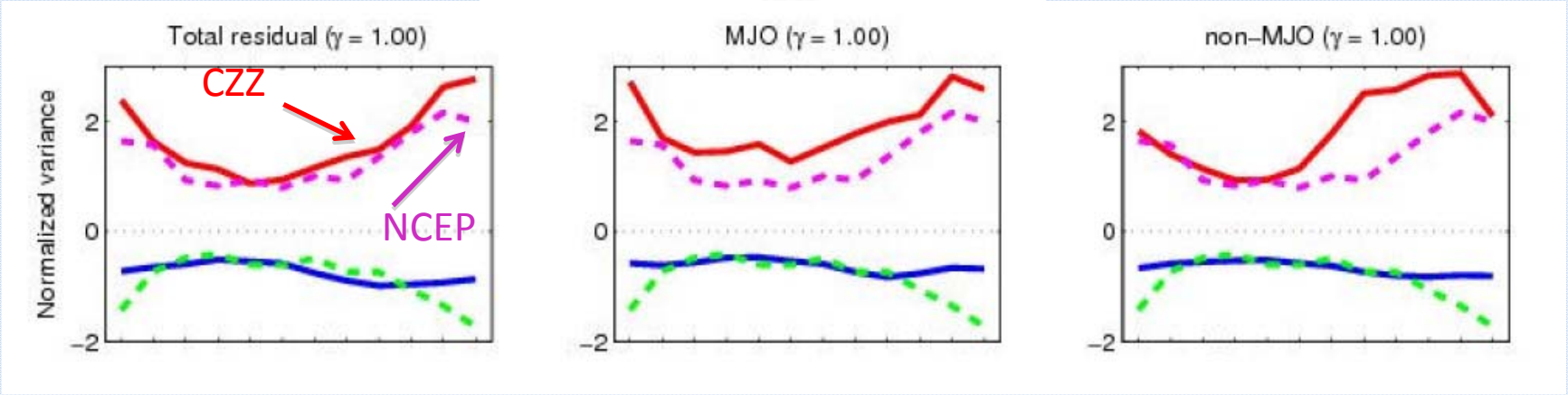

CZZ + BAMC SF

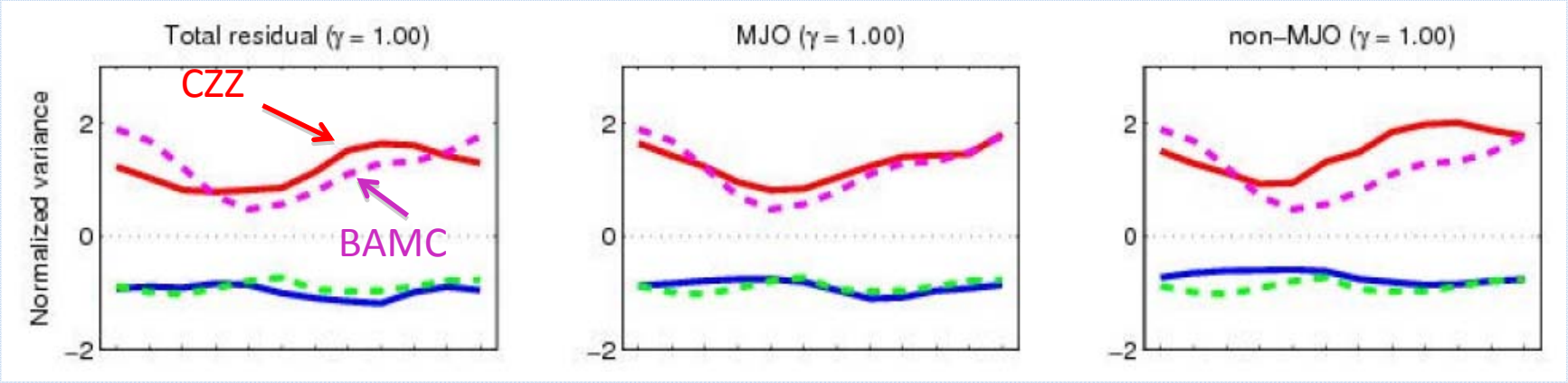

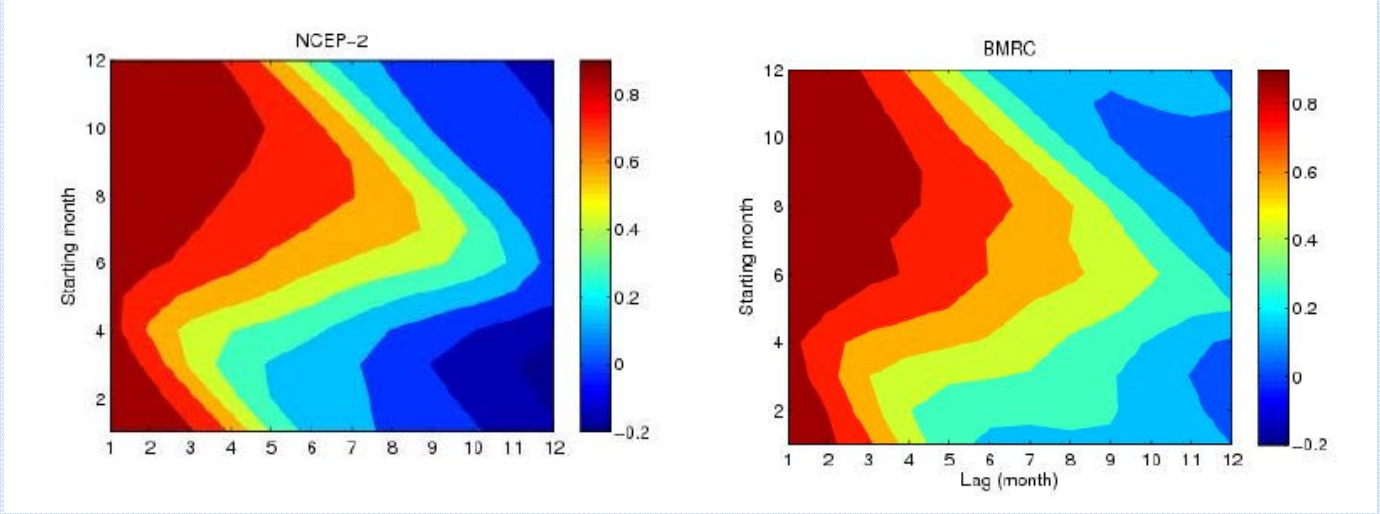

CZZ + NCEP SF

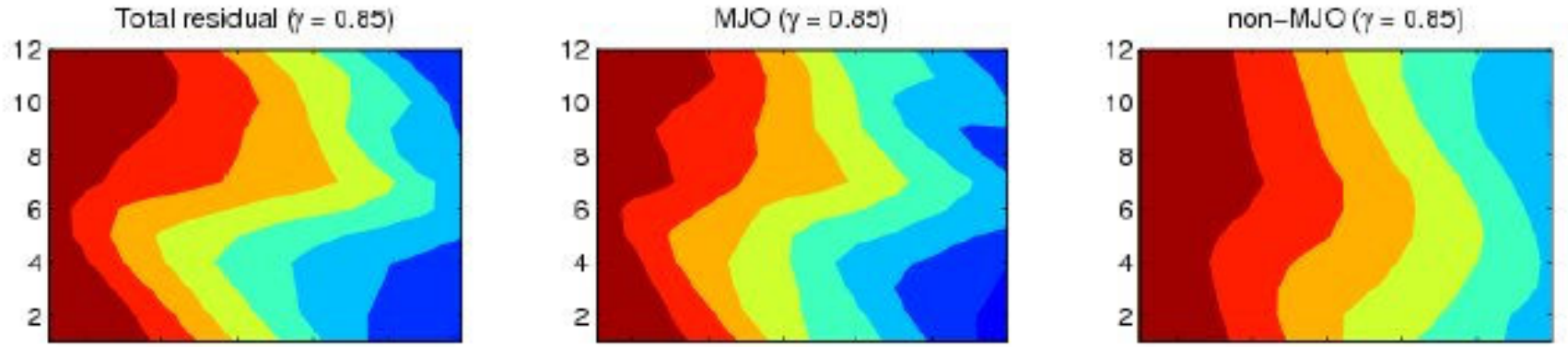

CZZ + BAMC SF

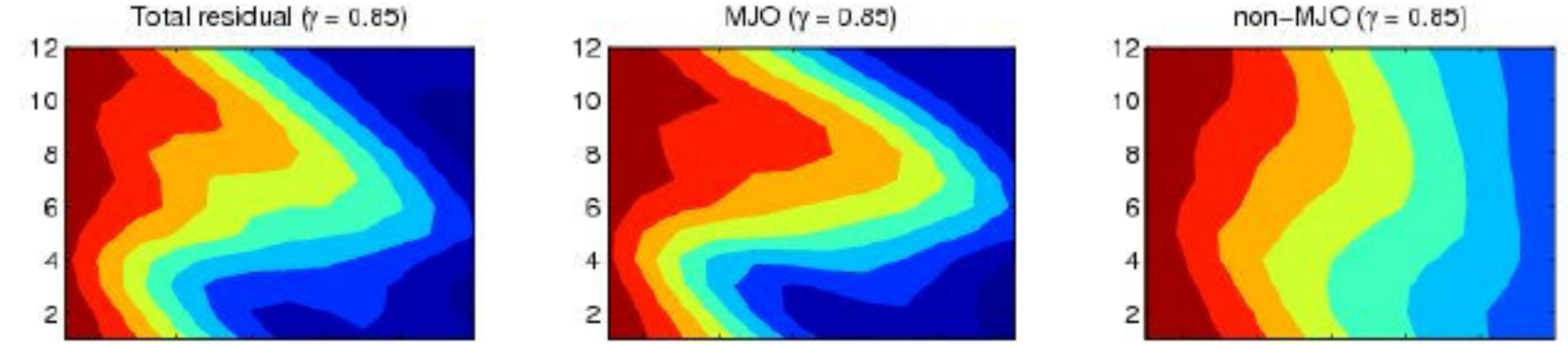

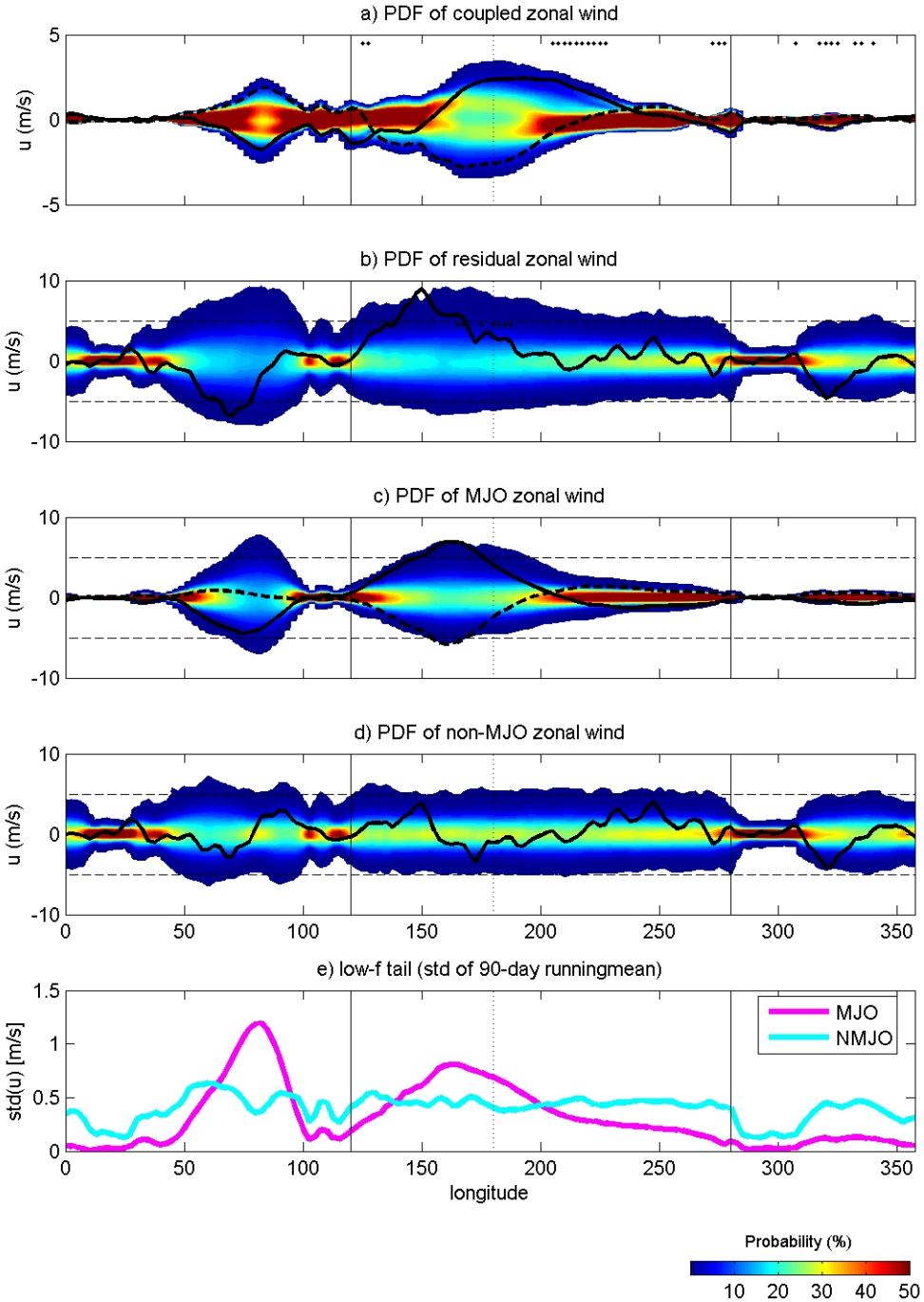

$\tau(SST)$

τ_f

τ_{MJO}

τ_{NMJO}

Kelvin-Wave Forcing:

$$K(x_0,t_0) = \int_0^{x_0} \tau_x\left(x, t_0 - \frac{x_0 - x}{c}\right) dx = K(\quad_x)$$

Kelvin-Wave Forcing by the MJO: $K(\quad_{MJO})$

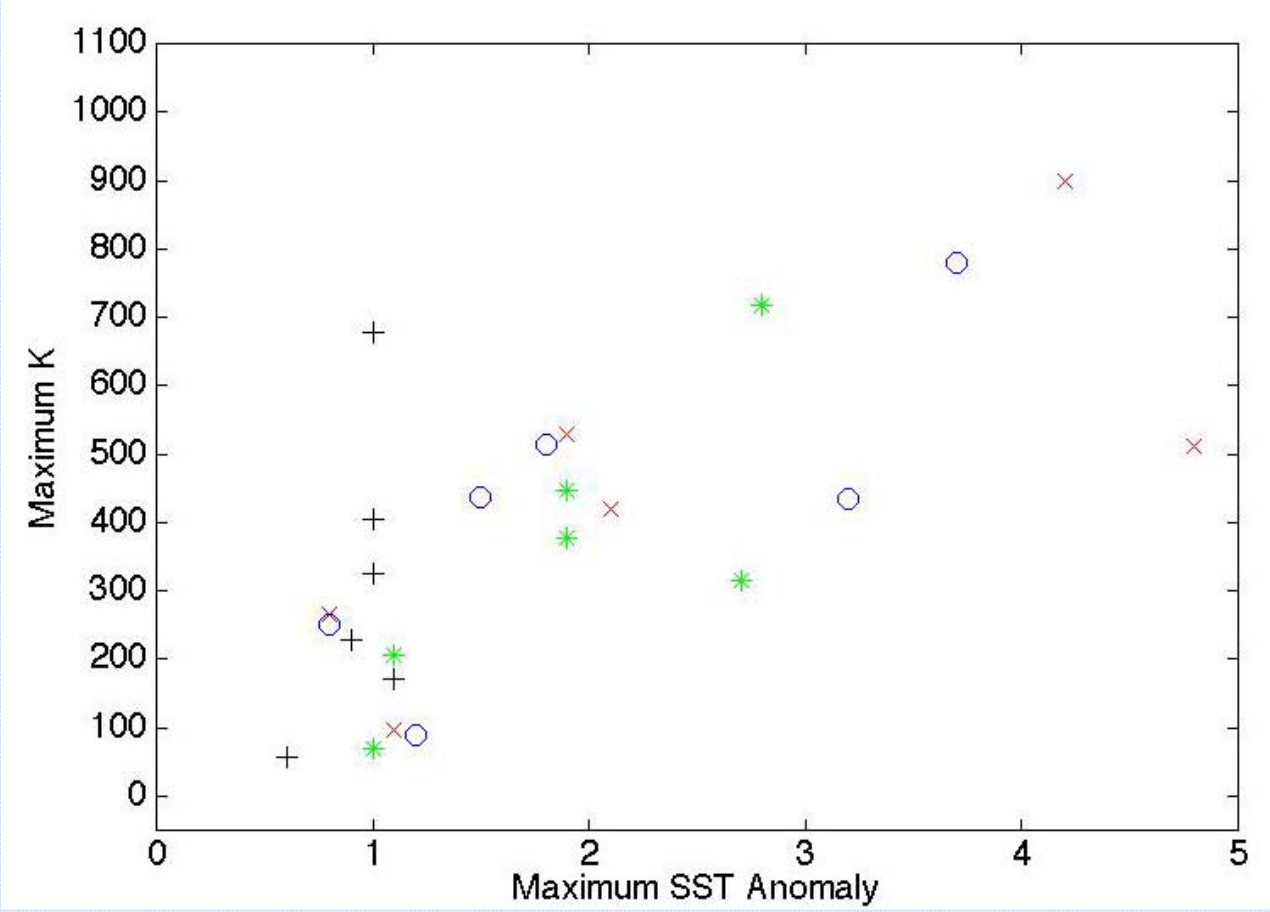

Oceanic Kelvin wave: reduction in equatorial upwelling

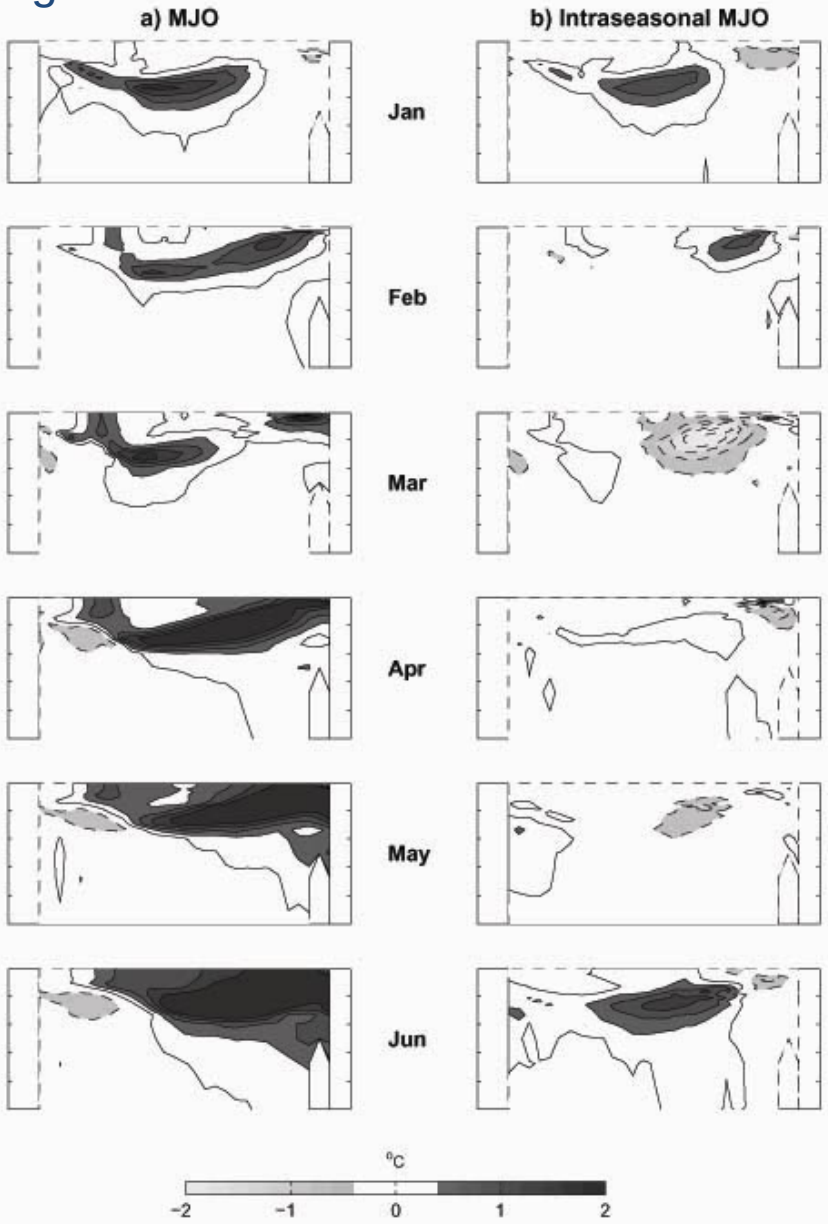

Zavala-Garay et al 2007

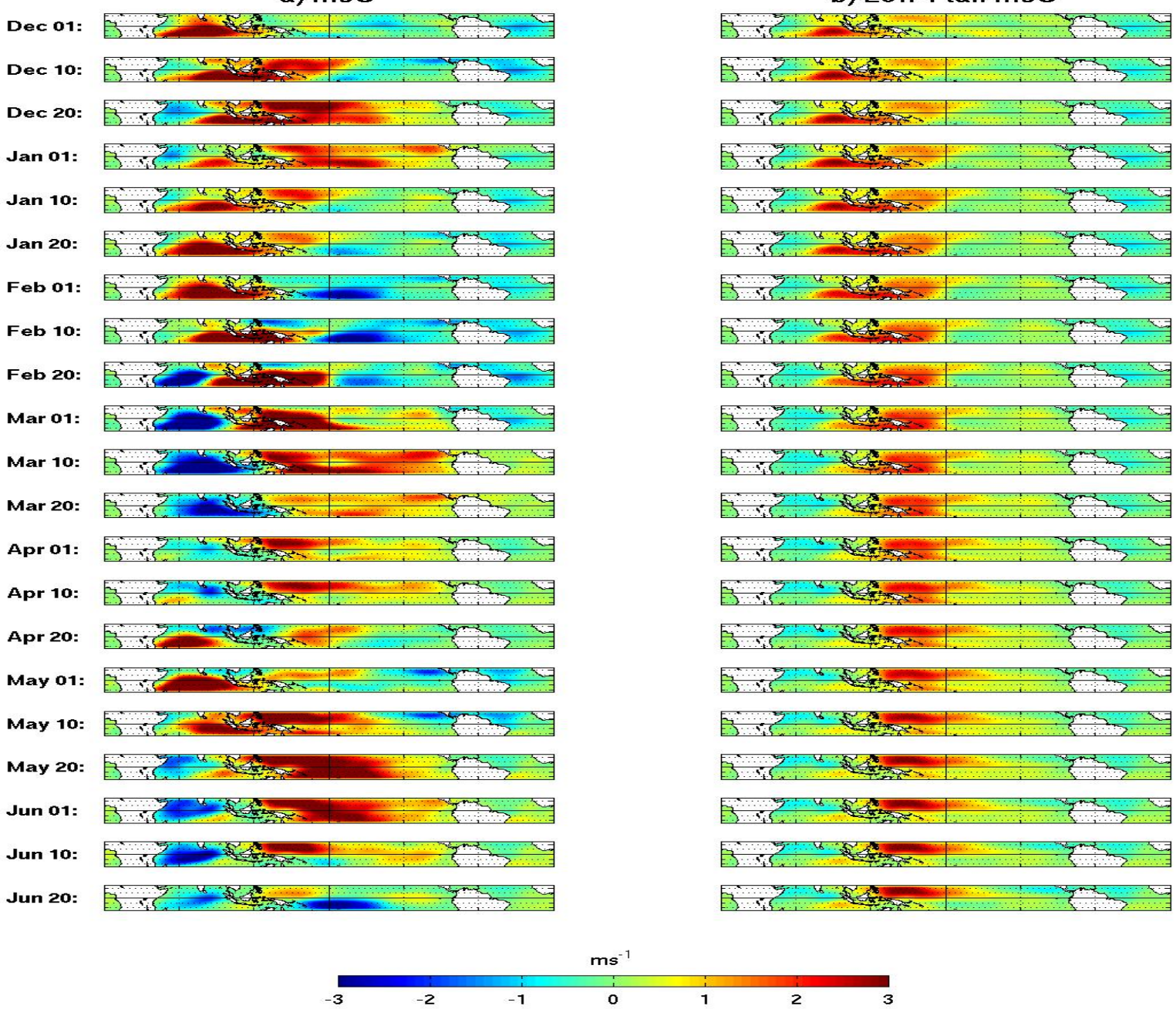
a) MJO
b) Low-f tail MJO
Dec 01:
Dec 10:
Dec 20:
Jan 01:
Jan 10:
Jan 20:
Feb 01:
Feb 10:
Feb 20:
Mar 01:
Mar 10:
Mar 20:
Apr 01:
Apr 10:
Apr 20:
May 01:
May 10:
May 20:
Jun 01:
Jun 10:
Jun 20:
ms-1
-3
-2
-1
0
1
2
3

Summary:

•Impacts of errors in model precipitation (or surface buoyancy flux) on tropical intraseasonal fluctuations in SST can be amplified by biases in the simulated MJO structure – mainly through the diurnal variability of the mixed layer;

•Atmospheric stochastic influences on ENSO depend on their spatial distributions and low-frequency (annual and interannual) components, which mainly come from the MJO.

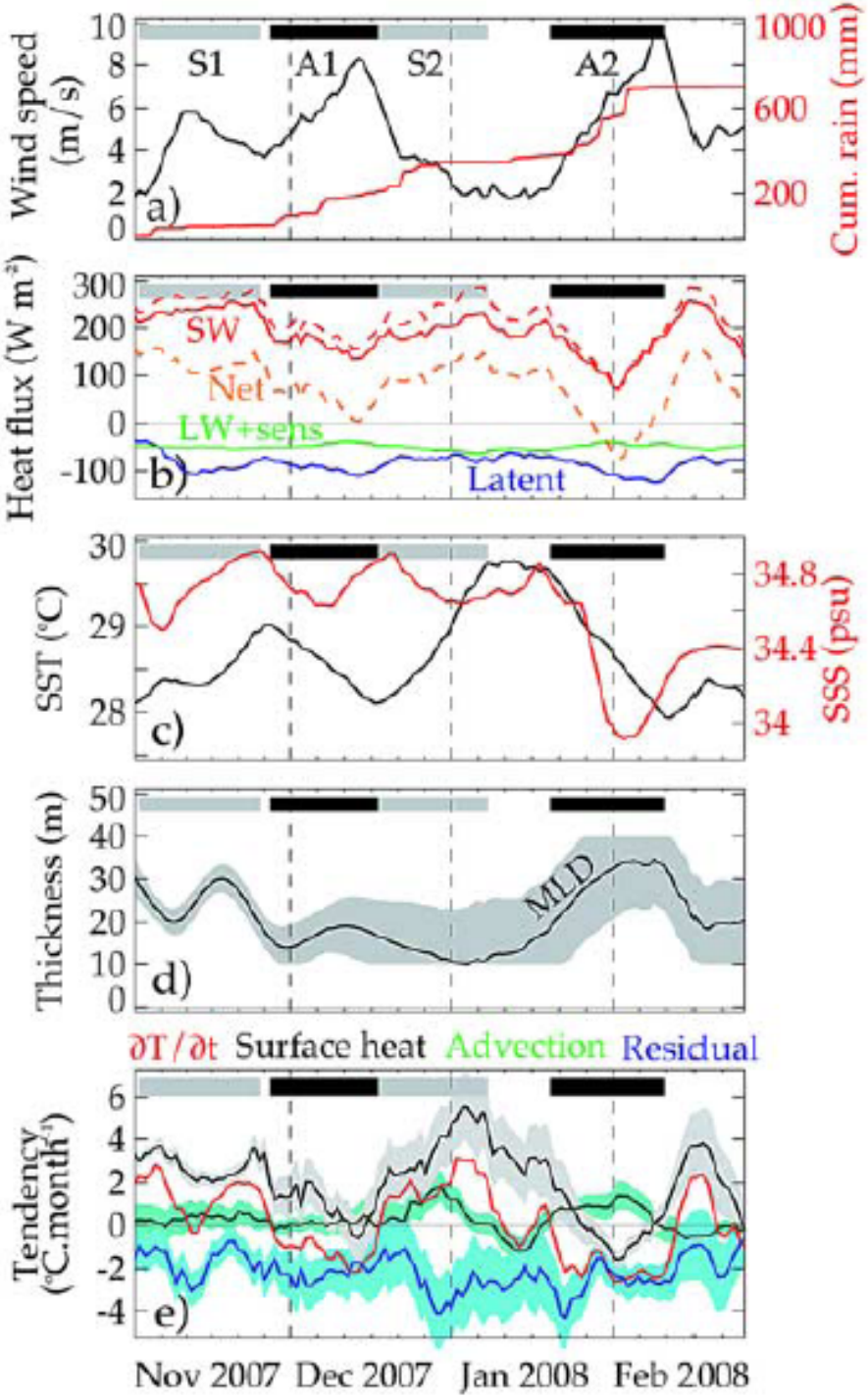
Wind speed (m/s)
Cum. rain (mm)
S1
A1
S2
A2
a)
Heat flux (W m⁻²)
SW
Net
LW+sens
Latent
b)
SST (°C)
SSS (psu)
c)
Thickness (m)
MLD
d)
∂T/∂t
Surface heat
Advection
Residual
Tendency (°C.month⁻¹)
e)
Nov 2007
Dec 2007
Jan 2008
Feb 2008

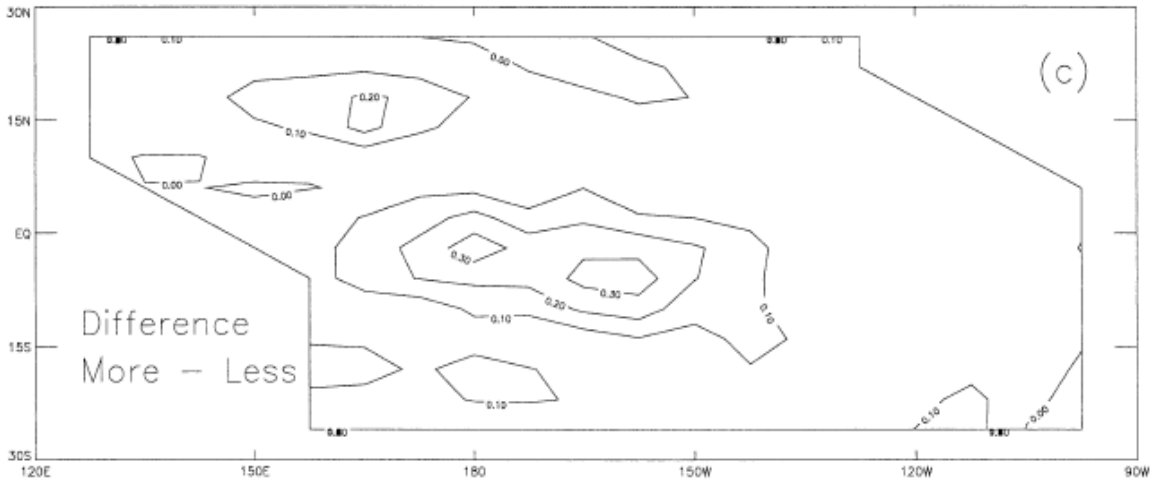

Difference between noise variance in zonal stress for periods of more and less predictable ENSO based on a prediction experiment by a coupled model of intermediate complexity in a linear stable dynamic regime. (From Flügle et al. 2004).

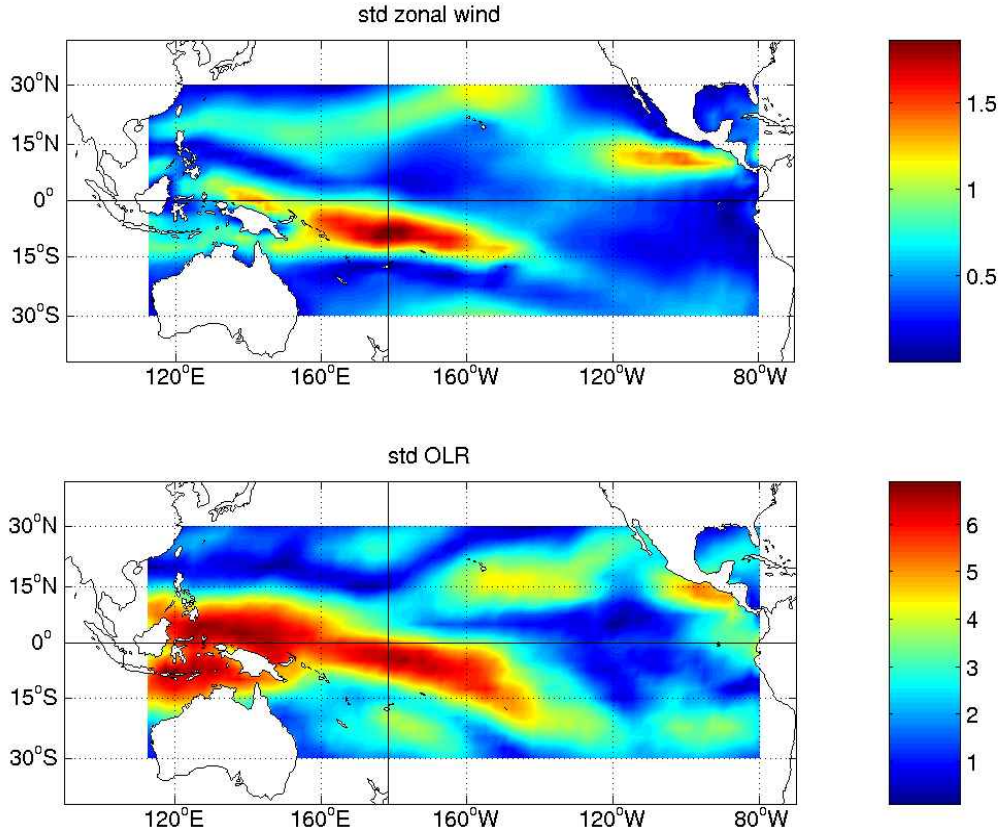

Distributions of MJO standard deviation derived from observed total stochastic forcing (courtesy of Javier Zavala)

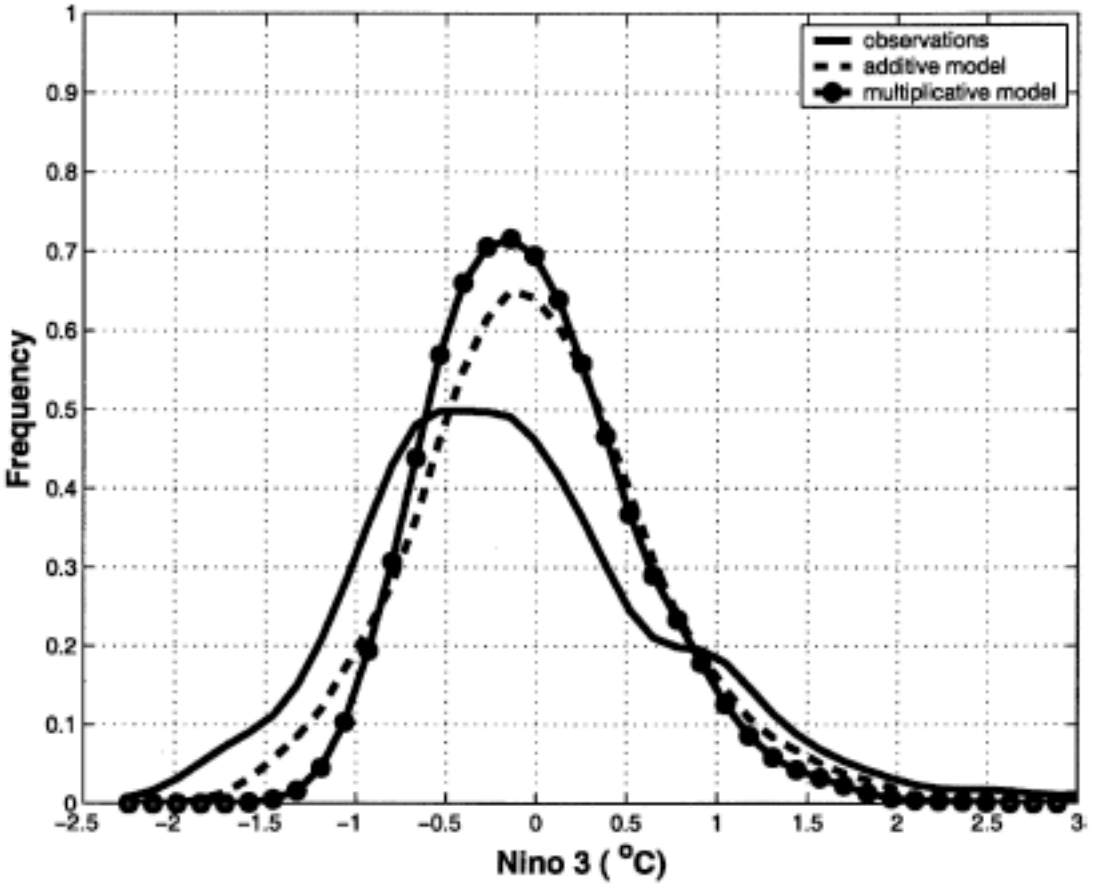

FIG. 12. PDFs of the observed 50-yr record of the Niño-3 index and the Niño-3 indices of the model run in both additive and multiplicative mode for 500 yr each time.

Perez et al. (2005)

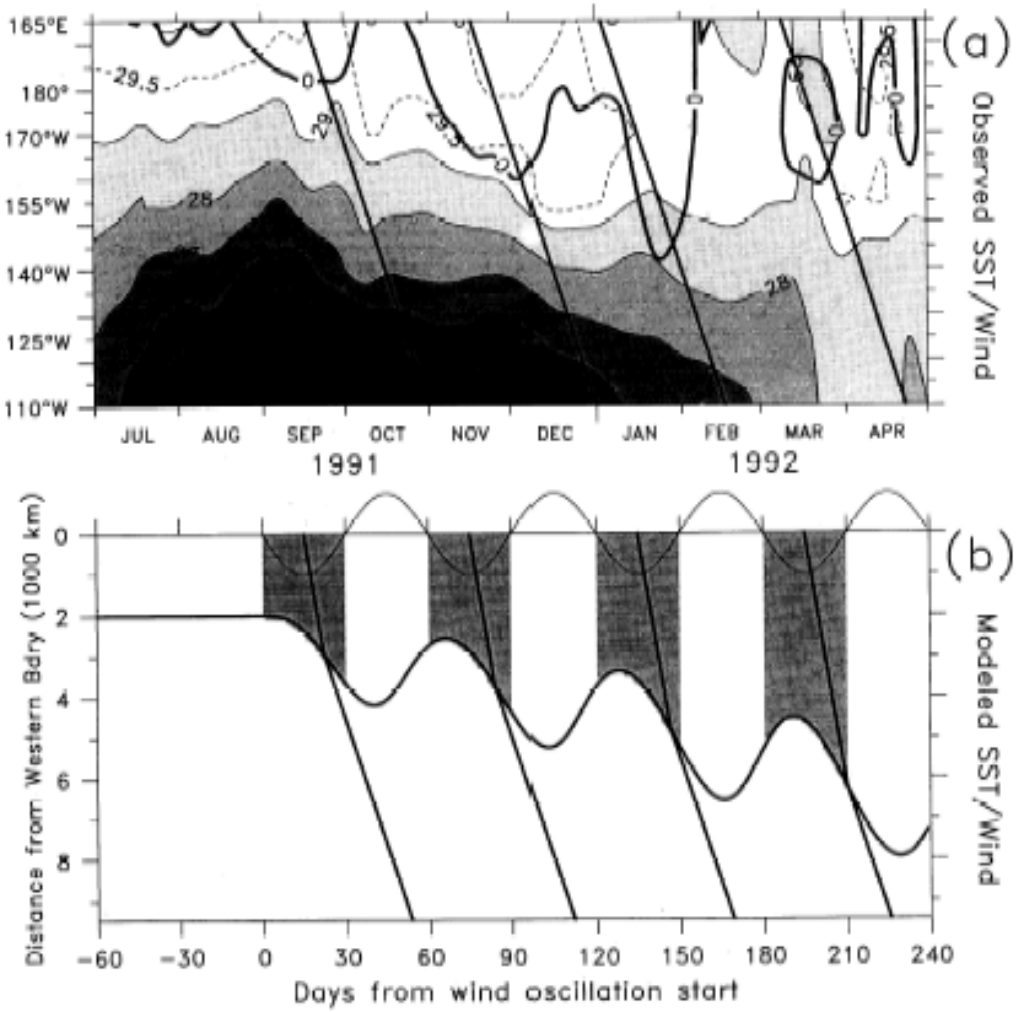

Figure 12. (a) Detail of SST on the equator for July 1991 through April 1992 (during the peak of the El Niño of 1991–1992). Contours and shading show SST with a contour interval of 1°C, with supplemental contour/shade at 29.5°C. Light contours show warmer temperatures (opposite of Figure 5). The heavy slant lines are the same Kelvin lines shown in Figure 3. The heavy contour labeled "0" is the zero line of zonal winds, showing the steplike progression of westerlies eastward over the Pacific during the onset of the warm event. (b) Model SST/wind to match the timing of Figure 12a. Output of the simple model described in section 4. The heavy curve is the eastern edge of the 29°C SST and the wind patch (the result of integrating (3): see text). The light sinusoidal curve at top is the time series of winds from (1) (up is easterly, down is westerly) (winds are zero before day 0). The shading shows the region of westerly winds. Slant lines indicate maximum positive pressure perturbation to match the observed Kelvin lines in Figure 12a; east of the forced region these are Kelvin characteristics, within the forced region they move at speed 2c (see text).

Kessler et al. 1995